SQUARE TILINGS OF SURFACES FROM DISCRETE HARMONIC 1-CHAINS

BY EDWARD DER-YU CHIEN

A dissertation submitted to the
Graduate School—New Brunswick
Rutgers, The State University of New Jersey
in partial fulfillment of the requirements
for the degree of
Doctor of Philosophy
Graduate Program in Mathematics

Written under the direction of
Professor Feng Luo
and approved by

_____

_____

_____

_____

New Brunswick, New Jersey

October, 2015

ABSTRACT OF THE DISSERTATION

Square Tilings of Surfaces from Discrete Harmonic 1-Chains

by Edward Der-Yu Chien

Dissertation Director: Professor Feng Luo

Works of Dehn [De] and Brooks, Smith, Stone, and Tutte [BSST] have noted a classical correspondence between planar electrical networks and square tilings of a Euclidean rectangle. In this thesis, a generalization of this result is proven for a closed, orientable surface Σ_g of genus $g \geq 1$ with a CW decomposition Γ, and a generic non-zero first homology class. From these data, a square-tiled flat cone metric on Σ_g is produced. The construction utilizes a discrete harmonic representative, and a discrete Poincaré-Hopf theorem is obtained in the process.

Similar results for non-generic non-zero homology class are also obtained where the metric and tiling are constructed on a surface of equal or lower genus. Additionally, we obtain similar constructions of square-tiled metrics on surfaces with boundary via modification of the harmonicity conditions. Finally, it is simple to obtain rectangle-tiled flat cone metrics with the extra data of a resistance function r on the edges of Γ, and the necessary changes are described.

Acknowledgements

This thesis has been the product of many people, some who have assisted directly, and others in more subtle ways. I would like to begin by acknowledging the academic guidance and support of my advisor, Prof. Feng Luo. He has been especially helpful with this thesis work, collaborating with me to clarify my ideas and prove the desired results. Outside of this work, he has been invaluable as a source of mathematical knowledge, and it has always been enlightening to learn from him. I'm thankful that I've had the privilege to do so over these past few years. In the same vein, I'd like to thank my academic siblings: Tian Yang, Priyam Patel, and Susovan Pal (and Julien Roger, though not technically a Luo student). It has been a joy to learn alongside them, and from them.

More generally, I would like to thank my close friends and family for their love and support, which has been vital in sustaining me though the hardships of doctoral study and young adulthood. I would like to thank Simao Herdade for his cheerful demeanor and kind soul, which brighten my life each day I see him. It has been a pleasure to have walked alongside you these years on *meu caminho*. I would like to thank Rachel Levanger for her friendship and support, especially this last semester. We've spent many hours together in the library, as well as on the cliffs, be they wood and plastic, or rock. Here's to hoping there'll be many more. Thanks are due to Michael Burkhart, whom I shared many an adventurous evening with while he was at Rutgers. His postcards and gifts from far-off lands have been welcome surprises and reminders of our friendship. My present roommates, Shashank Kanade and Moulik Balasubramanian, have been wonderful companions, and I am sad that we will no longer be living together soon.

I would be remiss not to mention the climbing community I have found at Rutgers. It

has become a passion of mine, and has allowed me to meet many wonderful friends. In particular, I'd like to thank the following partners of past and present: David Luposchainsky, James Haddad, Pawel Janowski, Gautam Singh, Iwen Chi, Ryo Maeda, Mike Lane, Anne Kavalerchik, and Jeremy Pronchik. Climbing with these people and (others) have served as a welcome break from my doctoral studies and many times, has allowed me to clear my head and proceed anew.

Another endeavor that has been a constant during these years has been A5, the department intramural soccer team. It has brought me closer with my colleagues, and I have enjoyed organizing it. It was captained by Catherine Pfaff before me, and I leave it now in the capable hands of Cole Franks and Matt Charnley.

It is true that there are many others that are due thanks, and so I apologize in advance for any omissions. This forgetfulness is a primary character flaw, that those mentioned above have been gracious enough to endure. Hopefully, you may do the same.

Finally, I would like to thank my parents and siblings. They serve as a mirror in which to view myself, and to remind me of my origins. In many ways, they know me better than I know myself, having seen me change over the decades. Their love is often unspoken, but is always clear to me.

Dedication

To Hai-Lung Chien and Ming-Der Chang,

whose work goes unappreciated far too often.

Table of Contents

Chapter 1

Introduction

Constructing geometric structures on surfaces from combinatorial data has a long history in geometry and topology. In this thesis, we introduce and investigate one such method that produces flat cone metrics on surfaces arising from square tilings.

1.1 A classical result

The first insight in this direction was made by Dehn [De] and expounded upon by Brooks, Smith, Stone, and Tutte [BSST]. These authors discovered a correspondence between planar electrical networks and square tilings of a rectangle. Here is an illustrative example:

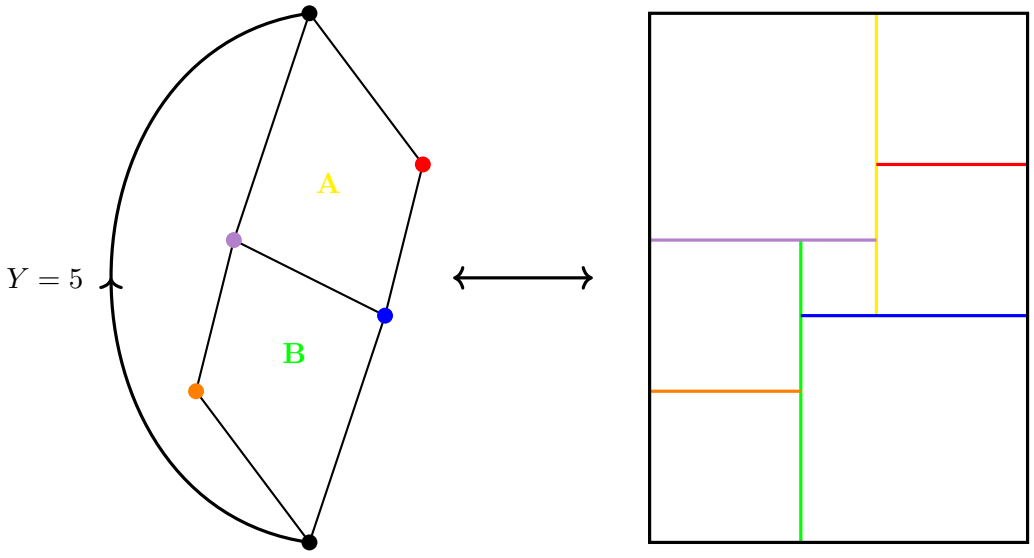

Figure 1.1

Let us begin with the simple definitions of a planar electrical network and a square

tiling of a rectangle.

Definition 1.1.1. A *planar electrical network* is a triple (G, b, Y) consisting of a planar, connected, directed graph G, a non-loop edge $b \in G$ to designate the battery edge, and a number $Y \in \mathbb{R}$ to denote the voltage to be applied over b.

In such a network, each edge is thought of as having unit resistance, giving us a unique circuit solution to Kirchhoff's laws. Letting E denote the set of edges of G, we denote this circuit solution with a function $c : E \setminus \{b\} \to \mathbb{R}$, describing the current through each edge. Note that the directions on the edges of the graph are suppressed in Figure 1.1 above. We also note that for the statement of their result, we will fix an embedding of G into the plane, such that b is a boundary of the exterior face.

Definition 1.1.2. A *square tiling of a rectangle* is a covering by squares with disjoint interiors, of a Euclidean rectangle with designated top, bottom, left, and right sides. Note that a square may also be a point, with empty interior.

With designated sides, we may also refer to horizontal and vertical line segments within such a tiling, which are connected subsets composed of the horizontal and vertical sides of the square tiles, respectively.

Let us briefly describe how a square tiling is *associated* with a planar network, and its circuit solution. In short, each resistor edge e corresponds to a square whose side length is the magnitude of the current through the edge. Furthermore, each vertex in the circuit corresponds to a horizontal segment, and each face with boundary made up of resistor edges corresponds to a vertical segment. Lastly, the positions of the squares and the segments with respect to each other reflect the topology of the network. In essence, the tiling becomes a nice visual representation of the circuit solution.

In Figure 1.1, the segment correspondences are color-coded, and the diagram serves as a clear example of these principles. The precise definition of a tiling being associated with a network has been deferred for the sake of brevity. It is given as Definition 2.4.1.

In [BSST], the authors' methods produce an associated square tiling for any planar

electrical network, proving the following theorem holds:

Theorem 2.5.1. **(Brooks, Smith, Stone, Tutte [BSST])** Given a planar electrical network (G, b, Y) with a unique circuit solution $c : E \setminus \{b\} \to \mathbb{R}$, and a fixed embedding of G in the plane, there is a unique associated square tiling of a rectangle of height Y and width I, the total current through the network.

1.2 Our generalization

In this thesis, the main result is an extension of Theorem 2.5.1 to the case of oriented, closed surfaces, following ideas of Calegari [Cal] and Kenyon. We consider a surface, Σ_g, of genus $g \geq 1$, with a CW decomposition Γ. If we consider a generic non-zero homology class $[\sigma] \in H_1^{\Gamma}(\Sigma_g, \mathbb{R})$ (the cellular homology with respect to Γ), it will have a unique discrete harmonic representative σ_h with non-zero coefficients for each edge. The edges of Γ may be thought of as being analogous to the planar network, while σ_h may be thought of as a local circuit solution.

From σ_h, a square-tiled flat cone metric is produced. An illustration of this metric for $g = 2$ and a particular CW decomposition is shown in the following diagram:

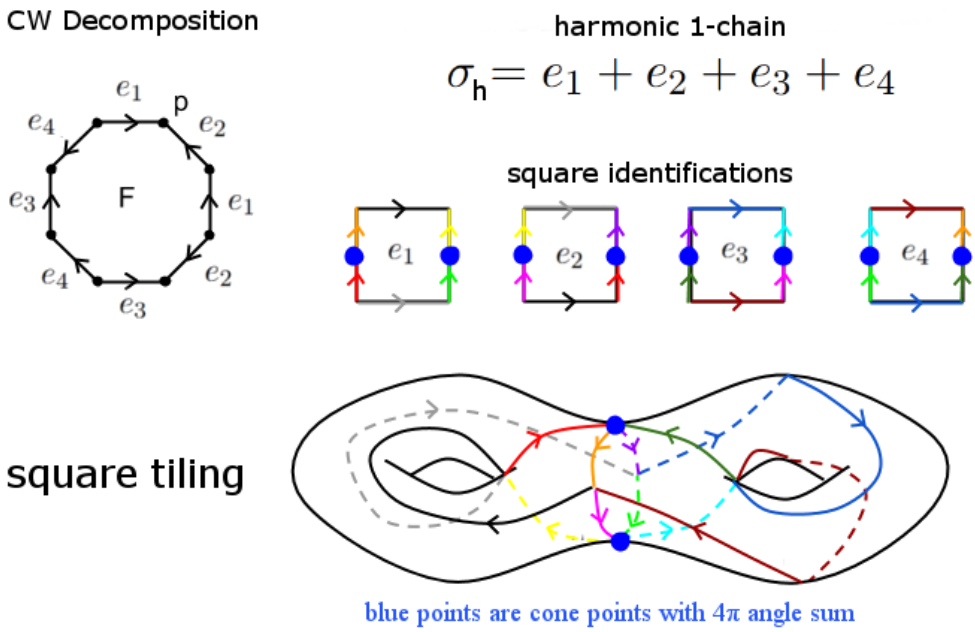

Figure 1.2

The tiling that is produced consists of *marked squares* which are Euclidean squares with designated top, bottom, left, and right sides. These sides are closed sets, so that a pair of sides may share a corner point. If a square s_i is in a tiling, then we denote these sides with s_i^t, s_i^b, s_i^l, and s_i^r, respectively. A marked square in a surface with a flat cone metric is defined to be the image of a continuous map on a marked square which is an isometric embedding on the interior. Again, we allow that a marked square s may be a point, with empty interior, in which case $s_i^t = s_i^b = s_i^l = s_i^r = s$.

Definition 1.2.1. A *marked oriented square tiling* of a flat cone metric d on a closed surface Σ_g is a covering by marked squares $s_1, s_2, \ldots, s_m$, with disjoint interior so that:

$$\bigcup_{i=1}^{m} s_i^t = \bigcup_{i=1}^{m} s_i^b \quad \& \quad \bigcup_{i=1}^{m} s_i^l = \bigcup_{i=1}^{m} s_i^r$$

In any such tiling, we again use the terminology of horizontal and vertical line segments to refer to connected subsets composed of the horizontal and vertical sides of the square

tiles. For any such tiling, the cone points of the flat cone metric d must have angles in $2\pi\mathbb{N}$, and branching of the horizontal and vertical segments in such a tiling can occur at these cone points.

Analogous to the classical case, there is a definition for a marked oriented square tiling to be associated with a discrete harmonic 1-chain σ_h. The precise statement is again deferred (Definition 3.2.1), but it may be easily described if we think of σ_h as designating a current flow along the edges of Γ. In particular, the coefficient c_i of each edge e_i may be thought of as describing the current flow along e_i. Then we again have the structural correspondences between edges, vertices, and faces of Γ and squares, horizontal segments, and vertical segments. Their relative positions again reflect the topology of Γ.

The result that we prove is below:

Theorem 3.3.1. Given a closed, oriented surface Σ_g of genus $g \geq 1$, a generic $[\sigma] \in H_1(\Sigma_g, \mathbb{R})\backslash\{0\}$, and a CW decomposition Γ with oriented edges, there exists a marked oriented square tiling of a flat cone metric d on Σ_g that is associated with σ_h, the unique harmonic representative of $[\sigma]$ in the cellular homology.

The generic condition on $[\sigma]$ merely requires that σ_h have non-zero coefficients c_i for each edge e_i.

The proof of the theorem is by construction, utilizing information from σ_h to identify marked squares along their boundaries by isometric orientation-reversing identifications. A slight modification of this construction allows for a simple proof of a discrete Poincaré-Hopf theorem. Lastly, the tiling and metric produced in the construction are just one of a family of such tilings and metrics. It is conjectured that this family forms a contractible $(2g-2)$-dimensional CW complex. Details of these statements and more are given in the third chapter.

Lastly, we'd like to make a note on interpretation of these results. The marked oriented square tiling gives rise to a holomorphic 1-form and a complex structure on Σ_g. This result, along with the classical one, may be viewed as discrete realizations of the intuition

of Klein, as cited by Poincaré [P]. He obtains a complex structure locally on a surface by identifying it with a metallic sheet and passing current through it. The current flow lines and equipotential lines at any point on the surface give locally orthogonal coordinates, and thus a complex structure.

1.3 Further generalizations

In the last chapter, we investigate further generalizations of Theorem 3.3.1, which we mention briefly here. First, we consider the non-generic case, where $[\sigma]$ has a harmonic representative σ_h with some zero coefficients. In this case, we may still perform our construction, but the resulting metric and marked oriented tiling lies on a surface S_σ of equal or lesser genus. To determine the topology, a canonical graph G_g related to Σ_g and Γ is investigated, along with particular connected subgraphs $\{H_j\}_{j=1}^{l}$ derived from the zero coefficients. Additionally, we need to include information about vertices incident only to edges with zero coefficients, and faces bounded only by edges with zero coefficients. We denote these sets with V_0 and F_0, respectively. Ultimately, we obtain a formula for the genus in terms of $|V_0|$, $|F_0|$, and the Euler characteristics, $\chi(H_j)$. The main result here is the following theorem:

Theorem 4.1.1. Given a closed, oriented surface Σ_g of genus $g \geq 1$, a non-generic $[\sigma] \in H_1(\Sigma_g, \mathbb{R})\backslash\{0\}$, and a CW decomposition Γ with oriented edges, there exists a marked oriented square tiling of a flat cone metric d on a surface S_σ of genus $g_0 \leq g$ that is associated with σ_h, the unique harmonic representative of $[\sigma]$. The genus g_0 is given by the formula:

$$g_0 = g + \frac{1}{2}\sum_{j=1}^{l}(\chi(H_j) - 1) + \frac{|V_0| + |F_0|}{2}$$

Secondly, we investigate modifying the harmonic condition at certain vertices and faces. In particular, we may ask that a 1-chain fail to be closed at certain vertices and co-closed on certain faces. Not all such conditions are achievable, but we determine which ones are, and define these conditions to be *modified harmonic* conditions. Given such conditions,

we again find an identification between such modified harmonic 1-chains and homological classes, and we denote the modified harmonic 1-chain with σ_{mh}. After performing our construction, this gives rise to boundary components for each vertex and face at which harmonicity fails, and we obtain square-tiled flat cone metrics on surfaces with boundary. In particular, we prove the following theorem:

Theorem 4.2.1. Given a closed, oriented surface Σ_g, a generic $[\sigma] \in H_1(\Sigma_g, \mathbb{R})\backslash\{0\}$, and a CW decomposition Γ with oriented edges, there exists a marked oriented square tiling of a flat cone metric d on $\Sigma_{g,n}$ that is associated with σ_{mh}, where n is the sum of the number of vertices and faces at which σ_{mh} fails to be harmonic.

The definitions for a marked oriented square tiling and for such a tiling to be associated to a modified harmonic 1-chain must be changed slightly in the case of surfaces with boundary. These are given in subsection 4.2.2.

Finally, it is simple to generalize our construction to obtain rectangular tilings with the additional data of a resistance function r on the edges of Γ. The resistance on each edge gives the aspect ratio of the corresponding rectangle. The statement of these results are simple adjustments to the theorems already stated, so we save them for the last chapter.

1.4 Related works and further studies

In this section, we quickly mention several related works that have informed and inspired us. Previously, one perspective on square tilings has been to view them as discrete vertex extremal metrics, as pioneered by Schramm [S] and Cannon, Floyd, and Parry [CFP]. In these works, a topological disc is triangulated and the boundary is partitioned into four segments (the designated top, bottom, left, and right), and vertex metrics realizing discrete extremal length are used to produce square tilings of the disc. Our initial investigations into generalizing this led to our current result. Interpretations of our resulting tilings in terms of discrete extremal vertex metrics would be of great interest.

Our work is also closely related with that of Hersonsky [H1, H2, H3, H4], which is

attempting to use rectangular tilings to approximate holomorphic maps. Our data is merely combinatorial at this point, but one might ask to incorporate geometric data via an appropriate choice of the resistances $r : E \to \mathbb{R}^+$. Hersonsky is nearing the completion of such a program for multiply-connected domains in the plane and has made initial steps toward doing this for surfaces.

There are also interesting investigations by Kenyon [K] in which he develops an invariant, which he calls the J-invariant, associated to a rectilinear polygon, which gives information about the square tileability of the polygon. He uses it to determine the square-tileable Euclidean tori and determines necessary conditions for square-tileability of surfaces. We plan to read this article carefully and see if our construction has anything more to say about such surfaces.

We would also like to acknowledge the ideas of Calegari [Cal], whose interpretations of Kenyon's pictures led us to the current result. He brings up some interesting questions about the image of our tiling construction, which we would like to investigate.

The work of Mercat [M1, M2] has previously investigated discrete harmonic 1-chains, and has tied them to the study of statistical physics. The connections between our work and his deserve further study.

Lastly, we note the potential for applications of our construction in the study of translation surfaces. These are flat cone metrics resulting from identification of plane polygons along parallel sides. By construction, our flat cone metrics are translation surfaces, resulting from identifications of squares or rectangles along parallel sides. We plan to investigate the extensive literature beginning with the following references: [Ma, MT, Z].

Chapter 2

Planar Electrical Networks and Square Tilings

In this chapter, we explain more fully the classical result in [BSST]. Recall that we consider a planar electrical network (G, b, Y), which has a unique circuit solution to Kirchhoff's laws $c : E \setminus \{b\} \to \mathbb{R}$. This function describes the current flow through each edge given voltage Y applied over edge b. We begin by stating explicitly these circuit laws.

2.1 Kirchhoff's laws

We note first that $c(e)$ may be negative, and that the sign of $c(e)$, in conjunction with the direction on e, describes the direction of current flow through the edge. In particular, if $c(e) > 0$, then current is flowing with the direction on e, and if $c(e) < 0$, then it is flowing against the direction on e. The directionality on each edge is an arbitrary choice to allow clear statement of the circuit laws. As most often stated, there are three of them:

2.1.1 Ohm's law

The simplest law states that for all non-battery edges $e \in E \setminus \{b\}$, we have that the voltage drop over the resistor is equal to the current times the resistance. Since we are assuming unit resistances, this law may be trivially satisfied by allowing current quantities to also represent the voltage drop quantities as they are the same. As mentioned in the introduction, with non-unit resistances, rectangle tilings result. The typical statement of Ohm's law is contained in subsection 4.3.1 where such tilings are discussed.

2.1.2 Current law

Consider a vertex v, which is not an endpoint of b, the battery edge. Let $\mathcal{I}(v)$ and $\mathcal{O}(v)$ denote the edges that end and start at v, respectively. The current law states that the incoming current is equal to the outgoing current for all such vertices:

$$\sum_{e \in \mathcal{I}(v)} c(e) = \sum_{e \in \mathcal{O}(v)} c(e)$$

2.1.3 Voltage loop law

Consider a simple loop γ in the undirected graph underlying G, so that edges in G may be traversed backward, from end point to start point. The battery edge b may also be in γ. Let $\mathcal{F}(\gamma)$ and $\mathcal{B}(\gamma)$ denote the edges that are traversed forward and backward, respectively.

The voltage loop law states that the voltage drops sum to 0 as γ is traversed. As we are considering unit resistances, voltage drops are merely current values for non-battery edges. For b, it adds a contribution of Y to one sum below, depending on the direction in which it is traversed. If $b \in \mathcal{F}(\gamma)$, let $\beta = 0$, and if $b \in \mathcal{B}(\gamma)$, let $\beta = 1$. Then the voltage loop law is expressed with the following formula:

$$(-1)^{\beta} Y + \sum_{e \in \mathcal{F}(\gamma) \setminus \{b\}} c(e) = \sum_{e \in \mathcal{B}(\gamma) \setminus \{b\}} c(e)$$

Note that this will also hold for loops γ that are not simple by adding the appropriate number of terms for edges that are traversed multiple times.

2.2 Existence and uniqueness of c

Let us briefly sketch an argument for existence and uniqueness of c, the circuit solution. This proof outline is from [CFP]. Let $|V|$ and $|E|$ denote the number of vertices and edges in G. Note that Kirchhoff's laws are all linear conditions on $|E| - 1$ variables, which take the values $c(e)$ for $e \neq b$. For the current law, we obtain $|V| - 2$ conditions from the current law, one for each vertex that is not an endpoint of b.

For the voltage loop law, there are an infinite number of conditions, as there are an infinite number of loops in G. However, there is a finite basis for the space spanned by these conditions. To obtain this basis, take a maximal tree T (with edges of G being viewed as non-directional) containing b as an edge. For every edge not in T, there is a voltage loop condition, and these conditions will be independent and generate the condition for any loop in G. This is left as a simple exercise for the reader.

We can express the cardinality of this basis of conditions by noting that G is homotopic to a wedge of S^1's, and the number of circles is equal to the number of edges not in T. Thus, a simple Euler characteristic calculation shows that there are $|E| - |V| + 1$ basis conditions.

As a result, we have $|E| - 1$ conditions to satisfy from Kirchhoff's laws and we see that finding c is equivalent to solving this nonhomogeneous square linear system (nonhomogeneity comes from assuming $Y \neq 0$). So, it will suffice to show that the kernel of our system is trivial, to get the desired result.

This corresponds to solving the system when $Y = 0$. In this case, suppose a solution has a non-zero current flow $c(e_i)$ on an edge e_i. Suppose that the flow along e_i does not end at a battery node. Then by the current law, there will be an edge from the same vertex with non-zero current flow away from that vertex. A similar argument will work for the starting vertex of the flow along e_i. In this way, we may construct a sequence of edges that have a consistent flow of current in one direction. The process will terminate when this flow starts and ends on the battery nodes. If it starts and ends on the same node, we obtain a contradiction of the voltage loop law. If it starts and ends on different nodes, then we may complete the loop with b and also obtain a contradiction, as we've assumed $Y = 0$.

2.3 Total current

Let us also quickly define the *total current* through the network, I, by looking at the terminal point of b, which we'll denote s_1. We will let $\mathcal{I}(s_1)$ and $\mathcal{O}(s_1)$ denote non-battery edges that have s_1 as a terminal point and starting point, respectively. Assuming Y is non-negative then:

$$I := \sum_{e \in \mathcal{I}(s_1)} c(e) - \sum_{e \in \mathcal{O}(s_1)} c(e)$$

If Y is negative, then we may take the negative of the above quantity.

2.4 Associated square tilings

Recall Definition 1.1.2 of a square tiling of a Euclidean rectangle. Recall also that horizontal and vertical line segments within such a tiling refer to connected line segments composed of the horizontal and vertical sides of the square tiles, respectively. Let us now give the precise definition of such a tiling being associated with a planar circuit network and its circuit solution c.

Definition 2.4.1. We say that a square tiling of a rectangle is *associated* to a circuit solution c of a planar electrical network if two sets of conditions are met. First, the following correspondences must hold:

1. Each resistor edge e corresponds to a square s_e with side length $|c(e)|$.
2. Each vertex v corresponds to a horizontal segment h_v with length $\sum_{e \in \mathcal{I}(v)} c(e) = \sum_{e \in \mathcal{O}(v)} c(e)$, the total current through v.
3. Each face f whose boundary consists of resistor edges, forming a simple loop denoted ∂f, corresponds to a vertical segment u_f with length $\sum_{e \in \mathcal{F}(\partial f)} c(e) = \sum_{e \in \mathcal{R}(\partial f)} c(e)$.

Secondly, the tiling must reflect the topology of G and the circuit solution. In the following conditions, recall that the sign of $c(e)$ in conjunction with the direction on e will determine the direction of current flow.

4. If an edge e carries current flowing out of (into) vertex v, then the bottom (top) side of s_e is contained in h_v.

5. If an edge e is carrying current clockwise (counterclockwise) about face f, then the right (left) side of s_e is contained in u_f.

We reproduce the example first presented in the introduction, for simpler digestion of this definition.

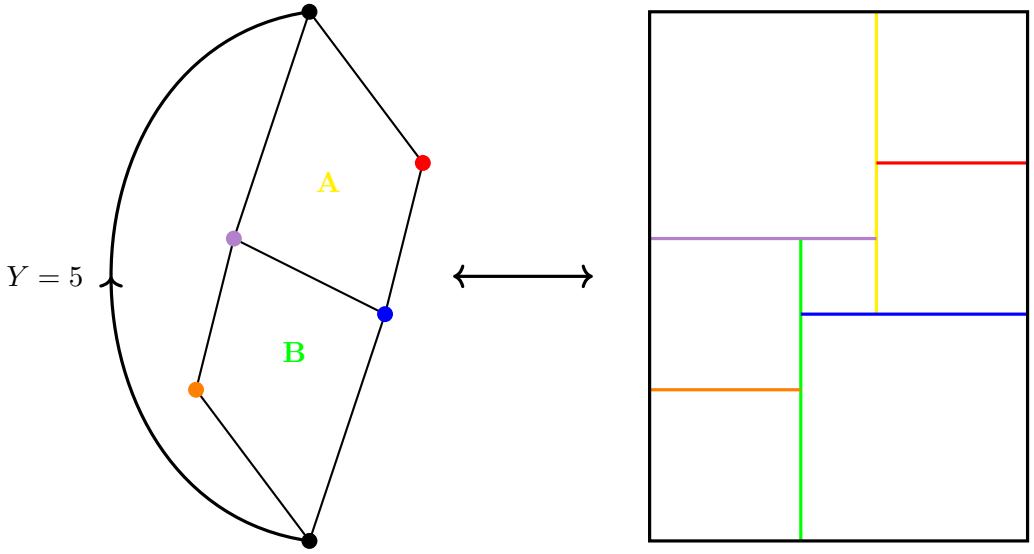

Figure 2.1

As noted before, the vertex and face correspondences of conditions 2 and 3 are color-coded in Figure 2.1. Then, the edge to square correspondence of condition 1 is implicitly clear with the second set of topological conditions.

2.5 The result

We restate the result from [BSST], first stated in the introduction:

Theorem 2.5.1. **(Brooks, Smith, Stone, Tutte [BSST])** Given a planar electrical network (G, b, Y) with a unique circuit solution $c : E \setminus \{b\} \to \mathbb{R}$, and a fixed embedding

of G in the plane, there is a unique associated square tiling of a rectangle of height Y and width I, the total current through the network.

Their basic method of proof involves giving coordinates for every square. The vertical coordinates are given by defining a voltage function on the vertices. For the horizontal coordinates, they define a dual network in the expected fashion with battery edge dual to the original battery edge. A potential is defined for this, giving these coordinates. For details, the reader is referred to [BSST].

Chapter 3

Generalization to Surfaces

Let us describe more fully, and present the proof of, our generalization of the classical result. Recall that we start with a closed, oriented surface of genus $g \geq 1$ and a non-zero homological class $[\sigma] \in H_1(\Sigma_g, \mathbb{R}) \backslash \{0\}$. Analogous to the network, we consider a CW decomposition Γ. There is then a unique harmonic representative $\sigma_h \in C_1^\Gamma(\Sigma_g, \mathbb{R})$ in the cellular homology with respect to Γ. Let us begin with a careful discussion of this fact.

3.1 Harmonicity

We start with the definition of harmonicity. Recall the typical setup for cellular homology and cohomology and the ∂ and δ operators. Coefficients in $\mathbb{R}$ are assumed, and the spaces below are for chains and co-chains in the cellular homology and cohomology of Σ_g with respect to Γ. This information will be assumed for the remainder of this section to simplify notation.

$$\begin{array}{ccccc} C_0^\Gamma & \xleftarrow{\partial} & C_1^\Gamma & \xleftarrow{\partial} & C_2^\Gamma \\ & & \downarrow \phi_1 & & \\ C_\Gamma^0 & \xrightarrow{\delta} & C_\Gamma^1 & \xrightarrow{\delta} & C_\Gamma^2 \end{array}$$

Let V, E, and F denote the vertices, edges, and faces (0-cells, 1-cells, and 2-cells) of Γ. Thus, $|V|$, $|E|$, and $|F|$ will be the dimensions of C_0^Γ, C_1^Γ, and C_2^Γ (and C_Γ^0, C_Γ^1, and C_Γ^2), respectively.

In the above diagram, we need to specify ϕ_1, an isomorphism between C_1^Γ and C_Γ^1. Let us index the edges arbitrarily $E = \{e_1, e_2, \ldots, e_{|E|}\}$, and let their dual elements in C_Γ^1 be denoted $e_1^*, e_2^*, \ldots, e_{|E|}^*$, where these elements are defined by the relation $e_i^*(e_j) = \delta_{ij}$.

This allows us to simply define $\phi_1(e_i) := e_i^*$ and extend to all 1-chains in C_1^Γ by linearity.

In addition, later on, we will need to refer to explicit ∂ and δ maps, so we give the edges and faces orientations derived from their explicit attaching maps. For the edges, the orientation we impose is arbitrary, but for the faces, we ensure that the orientations agree with a given orientation of Σ_g. With respect to this orientation, we will take the convention that the boundaries of the faces are to be traversed counterclockwise.

Definition 3.1.1. A 1-chain $\sigma \in C_1^\Gamma$ is *harmonic* if $\partial\sigma = 0$ and $\delta\phi_1(\sigma) = 0$. In other words, if σ is both closed and co-closed.

3.1.1 Harmonic 1-chain as local circuit solution

A harmonic 1-chain σ may be thought of as a local solution to Kirchhoff's laws. Let $\sigma = c_1 e_1 + \cdots + c_{|E|} e_{|E|}$, and we take the coefficients c_i, in conjunction with the directions on the e_i, to describe the current through each edge. Naturally, as in the classical case, if $c_i > 0$, then the current flows with the direction on e_i, and if $c_i < 0$, then the current flows against the direction on e_i.

Under this interpretation, we have that $\partial\sigma = 0$ corresponds to the current law holding at each vertex. In particular, if we have $\partial\sigma = a_1 v_1 + \cdots + a_{|V|} v_{|V|}$, where the v_j denote the vertices of Γ, then we may express the coefficient a_j as the total current through v_j. As in the classical case, we let $\mathcal{I}(v)$ and $\mathcal{O}(v)$ denote the edges that end and start at v, respectively.

$$a_j = \left(\sum_{e_i \in \mathcal{I}(v)} c_i \right) - \left(\sum_{e_i \in \mathcal{O}(v)} c_i \right)$$

Similarly, we have that $\delta\phi_1(\sigma) = 0$ corresponds to the voltage loop law holding around each face. If $f_1, f_2, \ldots, f_{|F|}$ denote the faces of Γ, let $f_1^*, f_2^*, \ldots, f_{|F|}^*$ denote the dual elements of C_Γ^2 that satisfy the relation $f_i^*(f_j) = \delta_{ij}$. Then we have that $\delta\phi_1(\sigma) = d_1 f_1^* + \cdots + d_{|F|} f_{|F|}^*$ for some coefficients d_k, and we may express these as the total current around f_k. As before, let $\mathcal{F}(\partial f)$ and $\mathcal{B}(\partial f)$ denote edges in the boundary of f that are

traversed forward and backward, respectively.

$$d_k = \left(\sum_{e_i \in \mathcal{F}(\gamma)} c_i \right) - \left(\sum_{e_i \in \mathcal{B}(\gamma)} c_i \right)$$

At this point, we make a remark about notation. For the remainder of the thesis, we will use c_i to denote the coefficient for edge e_i in a 1-chain σ, potentially without referencing the edge or 1-chain nearby in the text.

3.1.2 Unique harmonic representative

Now, let us show that each homological class has a unique harmonic representative:

Lemma 3.1.2. For a homological class $[\sigma] \in H_1^\Gamma(\Sigma_g, \mathbb{R})$, there is a unique harmonic representative σ_h.

Proof. Consider the inner product on C_1^Γ where the e_i form an orthonormal basis. This gives an orthogonal decomposition $C_1^\Gamma = \mathrm{im}(\partial) \oplus \mathrm{im}(\partial)^\perp$. Then for an arbitrary representative $\sigma \in [\sigma]$ we may consider it in this decomposition as $\sigma = \partial\alpha + \sigma_h$, where $\alpha \in C_2^\Gamma$. From this, it is clear that $\partial\sigma_h = 0$. To see that $\delta\phi_1(\sigma_h) = 0$, let us consider its value on any face f:

$$\delta\phi_1(\sigma_h)(f) = \phi_1(\sigma_h)(\partial f) = \langle \sigma_h, \partial f \rangle = 0$$

where the inner product is the same as the one inducing the orthogonal decomposition.

To show uniqueness, consider a different representative σ' for $[\sigma]$, with an orthogonal decomposition $\sigma' = \partial\alpha' + \sigma_h'$. Taking their difference we find that:

$$\sigma - \sigma' = \partial(\alpha - \alpha') + \sigma_h - \sigma_h'$$

As both σ and σ' are representatives of $[\sigma]$, their difference must lie in $\mathrm{im}(\partial)$, implying that $\sigma_h - \sigma_h' \in \mathrm{im}(\partial)$. As this difference also lies in $\mathrm{im}(\partial)^\perp$, it must be zero.

□

In our tiling construction, to be described shortly, we start with a square for each edge e_i and the absolute value of the coefficient $|c_i|$ will denote the side length. Thus, care must be taken with zero coefficients. For example, if $[\sigma] = 0$, then the harmonic representative is $\sigma_h = 0$, and there is no sensible corresponding tiling in this case. For this reason, we only consider non-zero homological classes. Generically, σ_h will have $c_i \neq 0$ for all edges e_i. This will be referred to as the generic case, and when there are zero coefficients, this will be referred to as the non-generic case. The generic case is treated in this chapter, with the non-generic case treated in the first part of the next chapter.

3.2 Associated square tilings of surfaces

Recall Definition 1.2.1 where we defined marked oriented square tilings. We make some remarks about the definition and describe how a marked oriented square tiling may be associated with a discrete harmonic 1-chain σ_h.

3.2.1 Definition remarks

In spirit, the second two set equality conditions state that the top sides of squares only intersect with the bottom sides of other squares and left sides of squares only intersect with the right sides of other squares. However, this is not strictly true, with this rule being violated at the corners of the rectangles and at the cone points of d, as is already clear in Figure 1.2. The definition, as it is given, allows for these exceptions.

Note that this interpretation of the set equality conditions also makes it clearer that the cone angles for any underlying flat cone metric of such a tiling must be in $2\pi\mathbb{N}$.

3.2.2 Associated tilings

Interpreting the coefficients of the discrete harmonic 1-chain as representing current through the edges of Γ, the definition of a tiling being associated to σ_h is nearly identical to that for the circuit solution to a planar electrical network, with the coefficient c_i replacing $c(e)$.

Just as in the planar case, horizontal and vertical line segments refer to connected subsets composed of the horizontal and vertical sides of the square tiles, respectively.

One important note to make here is that generically, the tiling and flat cone metric will reside on Σ_g, where σ_h is a discrete harmonic 1-chain with respect to Γ. However, this is not always the case. More specifically, for the non-generic case, the tiling and flat cone metric may be on a surface of lesser genus, which we prove in the next chapter. For this reason, we use S_g to denote the closed, oriented surface on which the tiling and metric reside, to differentiate it from Σ_g.

Definition 3.2.1. A marked oriented square tiling of a flat cone metric d on a surface S_g will be *associated* to σ_h if two sets of conditions are met. First, the following correspondences must hold:

1. Each edge e_i corresponds to a marked square s_i with side length $|c_i|$.
2. Each vertex v corresponds to a horizontal segment h_v with length $\sum_{e\in\mathcal{I}(v)} c_i = \sum_{e\in\mathcal{O}(v)} c_i$, the total current through v.
3. Each face f, with boundary loop denoted ∂f, corresponds to a vertical segment u_f with length $\sum_{e\in\mathcal{F}(\partial f)} c_i = \sum_{e\in\mathcal{B}(\partial f)} c_i$.

Secondly, the tiling must reflect the topology of Γ and σ_h. In the following conditions, recall that the sign of c_i in conjunction with the direction on e_i will determine the direction of current flow.

4. If an edge e_i carries current flowing out of (into) vertex v, then the bottom (top) side of s_i is contained in h_v.
5. If an edge e_i is carrying current clockwise (counterclockwise) about face f, then the right (left) side of s_i is contained in u_f.

Note that in this surface case, horizontal and vertical segments will become branched at the cone points with cone angle greater than 2π. We produce again the example from the introduction for added clarity.

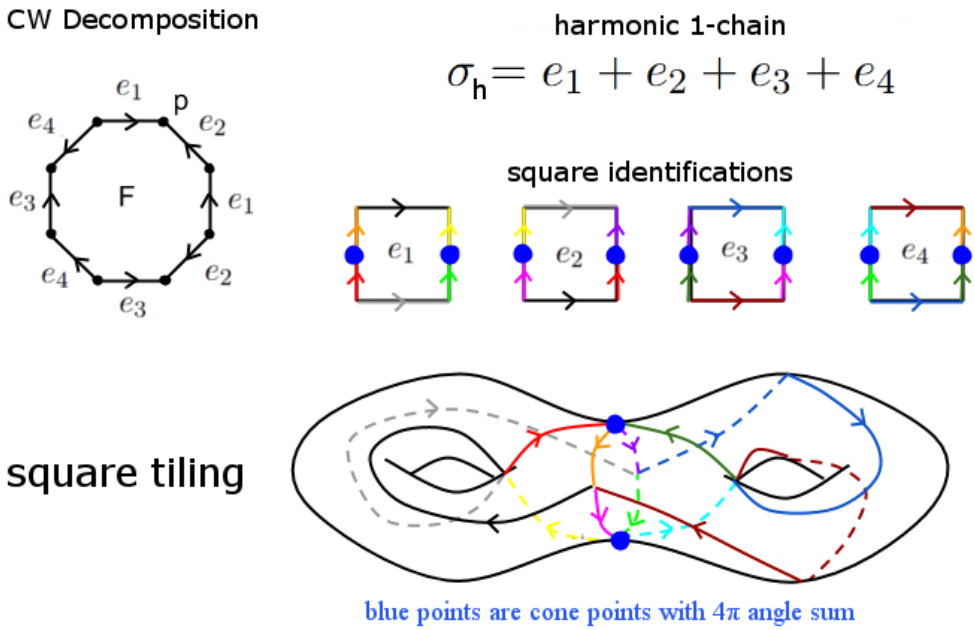

Figure 3.1

In this diagram, the colors do **not** color code any of the structural correspondences, but rather denote identifications to be made between the squares in the construction of the tiling and metric. The horizontal segment corresponding to the vertex is colored black, grey, blue, and maroon; while the vertical segment corresponding to the face is represented by the remaining colors. Note also that the squares are illustrated topologically, not geometrically, with four sides meeting at the blue cone points giving a total angle of 4π, though it looks otherwise. The branching phenomenon may be seen clearly at these points.

3.3 The result

Let us state our main result, for the generic case, as first stated in the introduction:

Theorem 3.3.1. Given a closed, oriented surface Σ_g of genus $g \geq 1$, a generic $[\sigma] \in H_1(\Sigma_g, \mathbb{R})\backslash\{0\}$, and a CW decomposition Γ with oriented edges, there exists a marked oriented square tiling of a flat cone metric d on Σ_g that is associated with σ_h, the unique harmonic representative of $[\sigma]$ in the cellular homology.

The proof of our theorem is given in the construction process for this tiling. For the remainder of this chapter, nearly all our 1-chains will be harmonic, so σ will be used to denote a harmonic 1-chain, as opposed to σ_h for the sake of simplicity.

3.4 Constructing $\hat{\Sigma}_g$ and d_σ

The first half of our construction process involves constructing a topological pinched surface, denoted $\hat{\Sigma}_g$, and assigning a metric d_σ to it. There is also the additional data of boundary loops, which is described.

3.4.1 Constructing $\hat{\Sigma}_g$

We first construct $\hat{\Sigma}_g$ which is associated with Σ_g and its CW decomposition Γ. Let us define a pinched surface:

Definition 3.4.1. A *pinched surface* is a Hausdorff topological space for which every point has a neighborhood which is homeomorphic to an open set in a cone over a finite union of intervals in $\mathbb{R}$.

For a pinched surface P, we will define the *boundary*, denoted ∂P, to be the set of points with no open neighborhood that is homeomorphic to $\mathbb{R}^2$. Points with open neighborhoods homeomorphic to an open neighborhood of the end cone point, are referred to as *pinch points*.

Now consider a *marked* disc D_i for each edge $e_i \in \Gamma$ with four distinct marked boundary points p_i^1, p_i^2, p_i^3, and p_i^4, labelled cyclically. Between any two points p_i^j and p_i^{j+1}, where the subscripts are considered modulo 4, there is a side of the disc, a boundary segment not containing other marked points. We denote this side with b_i^j. We will eventually embed

the interior of a marked square onto the interior of each disc D_i such that b_i^1 and b_i^3 will be vertical sides of the marked square, and b_i^2 and b_i^4 will be horizontal sides of the marked square.

Now, an identification between two marked points on D_i and D_j is made if edges e_i and e_j share a vertex as an endpoint and a face that they both border. The following diagram succinctly illustrates these rules, with the discs illustrated as squares, oriented such that p^1 is on the top right, p^2 is on the bottom right, p^3 is on the bottom left, and p^4 is on the top left:

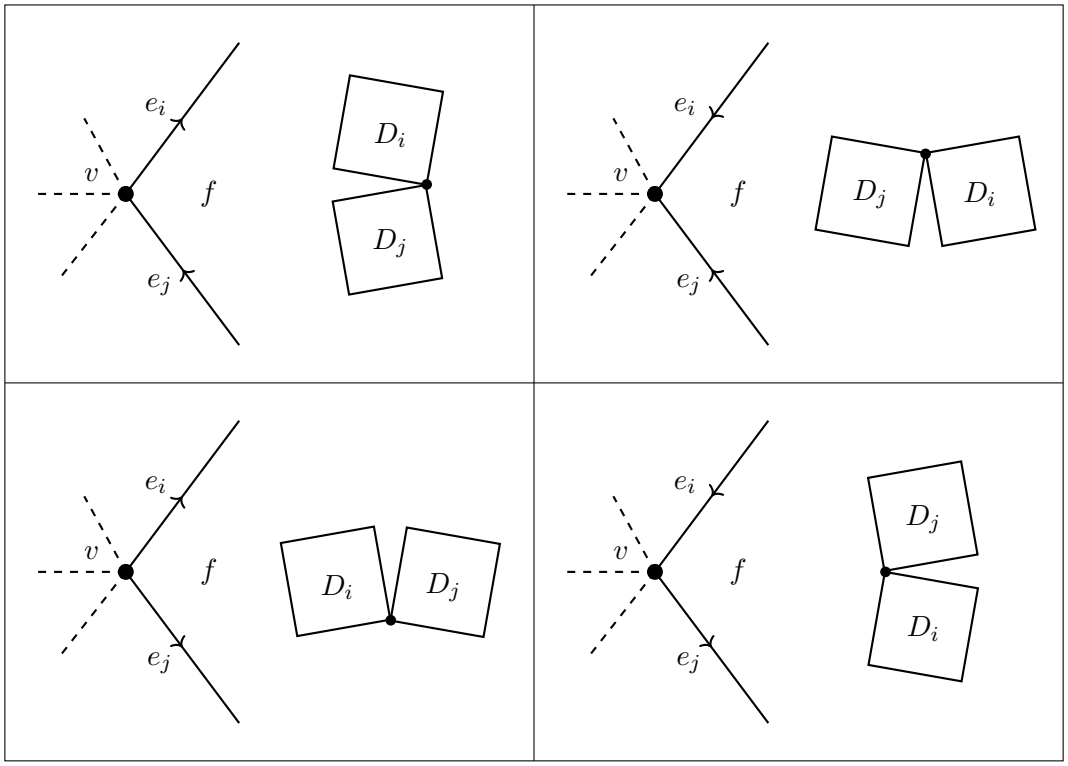

Figure 3.2: Identification rules

In words, the identification rules are:

1. If e_i starts from v and e_j ends at v, and both are directed clockwise about f, then we identify p_i^2 and p_j^1.

2. If both e_i and e_j end at v, and e_i is directed counterclockwise about f, then e_j

necessarily is directed clockwise about f, and we identify p_i^4 and p_i^1.

3. If both e_i and e_j start at v, and e_i is directed clockwise about f, then e_j necessarily is directed counterclockwise about f, and we identify p_i^2 and p_j^3.

4. If e_i ends at v and e_j starts at v, and both are directed counterclockwise about f, then we identify p_i^4 and p_j^3.

Note that if a vertex is of degree 1, or a face just has one boundary edge, then there will be self-identification of a marked disc. It is clear that the result of these identifications is a pinched surface, and we denote it with $\hat{\Sigma}_g$.

3.4.2 Assigning d_σ and s_i

After construction of $\hat{\Sigma}_g$, there is a simple assignment of a metric d_σ designated by our harmonic 1-chain. For each D_i, we give it the geometry of a Euclidean square of side length $|c_i|$. We also embed the interior of a marked oriented Euclidean square s_i of side length $|c_i|$ onto the interior of each disc, with the orientation specified by the direction of current flow along e_i.

If $c_i > 0$, so that current flow agrees with the given edge orientation, then b_i^1 will be s_i^r, b_i^2 will be s_i^b, b_i^3 will be s_i^l, b_i^4 will be s_i^t. If $c_i < 0$, so that current flow is opposite the given edge orientation, then the square will be flipped. In particular, b_i^1 will be s_i^l, b_i^2 will be s_i^t, b_i^3 will be s_i^r, b_i^4 will be s_i^b.

3.4.3 Boundary loops of $\hat{\Sigma}_g$

Lastly, there is additional data which consists of loops that cover $\partial\hat{\Sigma}_g$, one for each vertex and face of Γ. These loops are composed of the sides of the D_i. In particular, to each vertex v, we associate the tops and bottoms of the D_i corresponding to edges e_i carrying current to and from v, respectively. To each face f, we associate the left and right sides of the D_i corresponding to edges e_i carrying current counterclockwise and clockwise about f,

respectively. If we let p denote either a vertex or a face, we will denote the corresponding boundary loop with γ_p.

A diagram below illustrates an example of these loops for a vertex and a face. The local picture of the current flow along the edges of Γ is on the left, while the corresponding loops in $\hat{\Sigma}_g$ are on the right. On the left, the directions on the edges denote the direction of current flow, and may not reflect the direction on the edge. On the right, the loops are colored in blue, and the letters denote the type of the side that is in the loop.

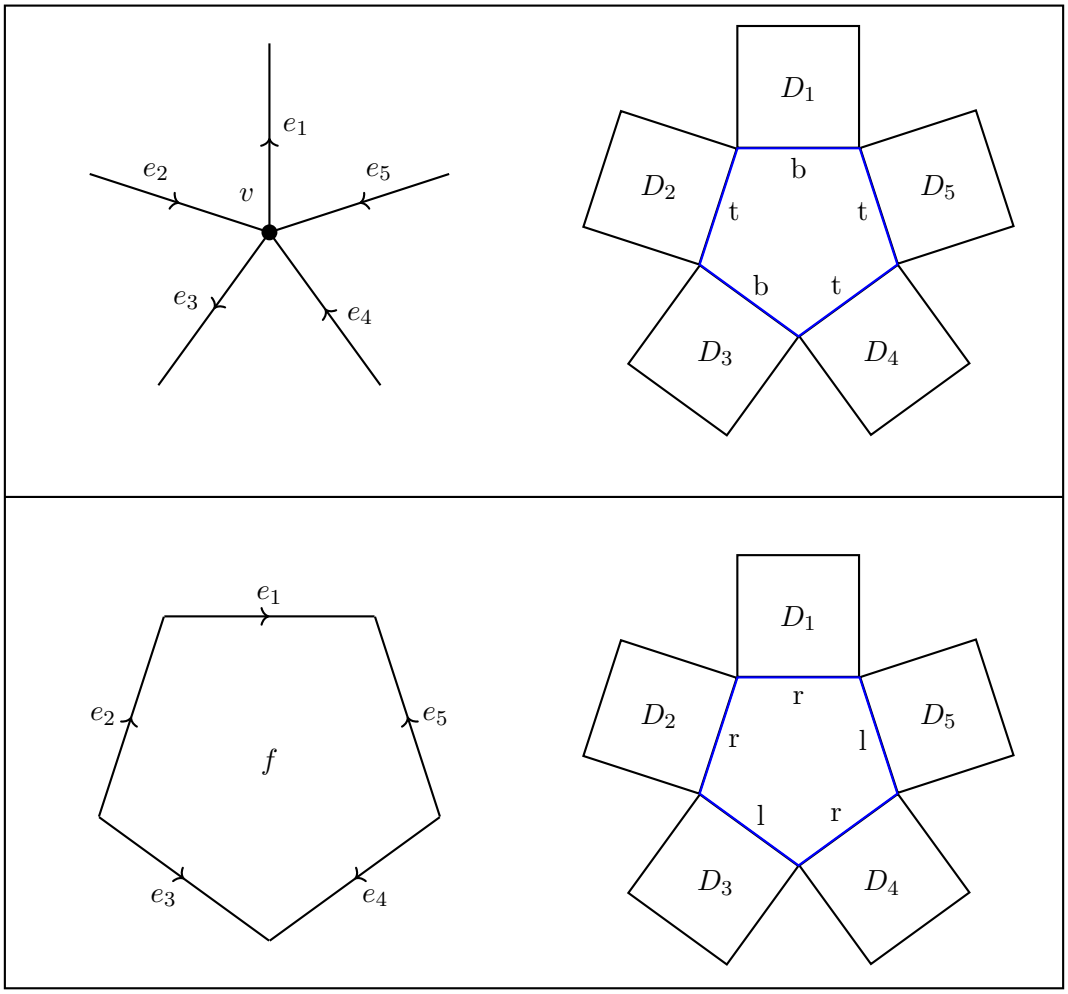

Figure 3.3: Boundary loop examples

Note that the loops will be disjoint, except for intersection at pinch points. At each

pinch point, it will be a face loop intersecting with a vertex loop, due to the nature of our identification rules.

3.5 Closing boundary loops

The second half of our tiling construction involves closing the boundary loops by isometrically identifying the s_i^t and the s_i^b at each vertex loop and the s_i^l and s_i^r at each face loop. This must be done in a way that does not introduce any genus. Precise definitions are made below.

3.5.1 Discrete index

We begin by defining the discrete index for a generic 1-chain τ about a vertex or face p, as it will play into our description of these identifications. In particular, note that in any γ_p in our construction, we may combine adjacent sides of the same type and group them into an even number of segments consisting of sides of the same type. More precisely, we make a CW decomposition of γ_p with an even number of 1-cells, such that each 1-cell consists of sides of only one type, and this type alternates as you traverse the loop.

The number of 1-cells is equal to the number of times that the direction of current flow changes as you travel cyclically around p. Let us denote this number with $scg_\tau(p)$. Note that this number makes perfect sense, even when τ is not harmonic. Then we may define the discrete index at p:

Definition 3.5.1. For a 1-chain τ and a vertex or face p, the *discrete index* at p is denoted $Ind_\tau(p)$, and is defined to be:

$$Ind_\tau(p) := 1 - \frac{scg_\tau(p)}{2}$$

Note also that as τ is generic, we have that $scg_\tau(p)$ is a positive even integer, implying that $Ind_\tau(p)$ is a non-positive integer.

3.5.2 Loop closings

Now, let us define precisely what it means to close a boundary loop. Let $l_1, l_2, \ldots, l_{2n}$ denote the 1-cells in γ_p mentioned above (so that $2n = scg_\sigma(p)$), and let $|l_1|, |l_2|, \ldots, |l_{2n}|$ denote their lengths under d_σ. They are labelled in a cyclic order, with an arbitrary start segment, so that the segments with even index will be of one type, and the segments with odd index will be of another type. Note that as σ is harmonic, we will have that $|l_1| + |l_3| + \cdots + |l_{2n-1}| = |l_2| + |l_4| + \cdots + |l_{2n}|$.

Definition 3.5.2. A *loop closing* of a boundary loop γ_p will be a further decomposition of the $\{l_i\}_{i=1}^{2n}$ into 1-cells $\{t_j\}_{j=1}^{2m}$, and a pairing of these 1-cells of opposite type, designating an orientation-reversing isometric identification of paired segments.

As mentioned previously, such identifications may introduce extra genus to our surface, so we consider only those that do not do this. In particular, let us embed γ_p in $\mathbb{R}^2$ as the boundary of a disc centered at the origin, and remove the interior of said disc, and consider the resulting topology when the identifications are made.

Definition 3.5.3. A *valid closing* of a boundary loop γ_p will be a loop closing which results in a space with the topology of $\mathbb{R}^2$, when γ_p is embedded as suggested above.

We mention two equivalent conditions briefly. The first is that the image of γ_p be a metric tree under the quotient map of the identification. The second is that if two pairs of points (x_1, x_2) and (y_1, y_2) on γ_p are identified, then the lines between them must not cross when considered in the embedding into the plane.

For better digestion of this definition, we present diagrams of two examples of valid closings. The boundary loops come from our genus 2 example, first presented in Figure 1.2. The top half presents the boundary loop and the image of the loop after a valid closing for the vertex loop. The bottom half presents the corresponding objects for the face loop. The boundary loops are on the left, and are in blue, while the images (metric trees) under identification are shown on the right. Further explanation follows the figure.

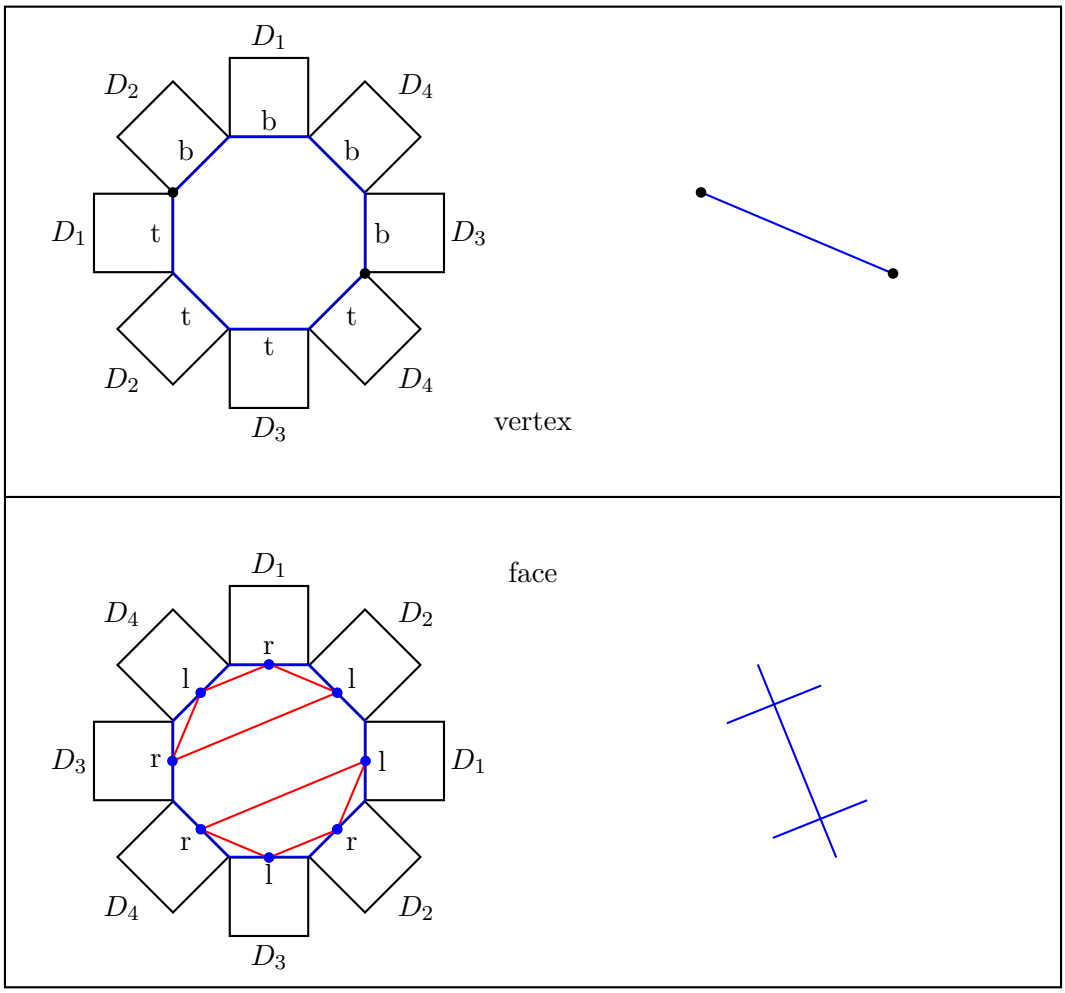

Figure 3.4: Valid closing examples

On the illustration of the boundary loop for the vertex, we have two black vertices, which represent the 0-cells in the CW decomposition of the loop into 1-cells of different types. The images of these vertices are also drawn in the image under identification on the right.

For the illustration of the boundary loop for the face, we have 8 blue vertices, joined by red lines. These red lines denote identifications of the endpoints. These blue vertices are 0-cells of the further decomposition that defines the valid closing (though they are not all of them). The further identifications are implicit and the image metric tree is shown

to the right.

As shown in this example, we note that there may be multiple valid closings for γ_p, depending on the index at p. If the index is 0, the closing is unique, with a simple pairing of l_1 and l_2 being the unique valid closing. This is shown in the example above with the vertex loop. When the index is negative, this uniqueness disappears. This is hinted at in the example with the face loop above. The conjectures in the final section of this chapter address this loss of uniqueness.

3.5.3 Existence of valid closings

For now, we demonstrate existence of a valid closing for any boundary loop:

Lemma 3.5.4. For any boundary loop γ_p arising from a harmonic 1-chain σ, there exists a valid closing.

Proof. Existence may be shown simply with the following algorithm, which simultaneously decomposes the segments $\{l_i\}_{i=1}^{2n}$ and pairs the resulting 1-cells. Indices are considered modulo $2n$ (so that $l_{2n+1} = 1$ and $l_0 = l_{2n}$).

1. Consider a shortest segment l_i and decompose it into halves t_{i_-} and t_{i_+}, where t_{i_-} intersects l_{i-1} and t_{i_+} intersects l_{i+1}.

2. Decompose l_{i-1} into two segments, one of which is of length $\frac{|l_i|}{2}$ and is adjacent to l_i.

3. Decompose l_{i+1} into two segments, one of which is of length $\frac{|l_i|}{2}$ and is adjacent to l_i.

4. Pair t_{i_-} with the segment from step 2, and pair t_{i_+} with the segment from step 3, identifying them.

5. Consider a new loop where the segments identified in the previous step are removed, and the other segments from steps 2 and 3 are combined. This new loop has two fewer

segments, and the lengths of these new segments will be $|l_1|, |l_2|, \ldots |l_{i-2}|, |l_{i-1}| + |l_{i+1}| - |l_i|, |l_{i+2}|, \ldots |l_{2n}|$.

6. Repeat steps 1-5 $(n-1)$ more times, changing the loop under consideration according to step 5 each time.

In step 1, choosing the shortest segment ensures us that l_{i-1} and l_{i+1} have enough length to be decomposed into two segments, one of which will be identified with half of l_i. Also, it is clear that for step 5, in the new loop formed, the sum of the lengths of the odd segments are equal to the sum for the even segments, as equal amounts of odd and even segments are identified and removed. Full identification occurs after n total runs through steps 1-5, as each iteration reduces the number of segments by 2.

It is clear that in the original loop γ_p that no two pairs of identified points have lines that cross when embedded in the plane, so we have a valid closing. □

3.5.4 Obtaining S_σ and the associated tiling

Given existence of these valid closings, we simply apply them to each boundary loop with the algorithm above. The result will be a marked oriented square tiling of a closed surface, which we denote with S_σ. In the construction, it is clear that the interiors of the squares are disjoint, and the set union conditions will hold as each side of a square is decomposed, with each piece identified to another of the opposite type.

Furthermore, it is clear that the tiling will be associated to our harmonic 1-chain σ. For the structural correspondences, we already have a square for each edge of the right size. The horizontal segment corresponding to any vertex v is the image of γ_v under the identification. The vertical segment corresponding to any face f is the image of γ_f under the identification. The topological conditions are automatically satisfied through our construction.

3.6 Proof of desired topology

To finish the proof, let us argue that S_σ is homeomorphic to Σ_g. For this we use a simple topological fact about finite 2-dimensional CW complexes.

Lemma 3.6.1. For X, a finite 2-dimensional CW complex, and a subcomplex A whose complement is a disjoint union of n open discs, we have that:

$$\chi(X) = \chi(A) + \chi(X \setminus A) = \chi(A) + n$$

Proof. Consider a CW decomposition of X formed by augmenting the subcomplex A, with the attachment of the n complementary discs along their boundaries, specified by their position in X. These attaching maps are guaranteed to have image within the 1-skeleton of A, as $A \cap \overline{X \setminus A} = \partial A$ (A is closed) and ∂A must be within the 1-skeleton of A. It is clear that the attachment of the n discs contributes n 2-cells to the alternating count for the Euler characteristic, so the result holds. □

It is clear that this generalizes to n-dimensional finite CW complexes, but we only state this version here, as it is all we need. Now, for the desired result:

Lemma 3.6.2. S_σ is homeomorphic to Σ_g.

Proof. Consider that S_σ is homotopic to the space obtained by gluing discs into the boundary loops of $\hat{\Sigma}_g$. In particular, the valid closing process is topologically the same as gluing in a disc for each vertex and face.

We may now use Lemma 3.6.1 directly, with X being the space homotopic to S_σ and $A = \hat{\Sigma}_g$. As before, we let $|V|$, $|E|$, and $|F|$ denote the number of vertices, edges, and faces in Γ. It is clear that $X \setminus A$ consists of $|V| + |F|$ open discs.

For the Euler characteristic of $\hat{\Sigma}_g$, there is an obvious CW decomposition, where each D_i is a 2-cell, each side of a disc D_i is a 1-cell, and each pinch point is a 0-cell. Thus, in this decomposition, there are $|E|$ 2-cells and $4|E|$ 1-cells. For the 0-cells, we note that

in constructing $\chi(\hat{\Sigma}_g)$, before we identify the D_i, we have $4|E|$ 0-cells from the marked points on the discs. Each identification creates a pinch point and quotients together two of these 0-cells. The total number of identifications is equal to the sum of the degrees of the vertices in Γ which is just $2|E|$. Thus, there are $4|E| - 2|E| = 2|E|$ vertices in this CW decomposition and $\chi(\hat{\Sigma}_g) = E - 4|E| + 2|E| = -|E|$.

Thus, we find ultimately that $\chi(S_\sigma) = -|E| + |V| + |F| = \chi(\Sigma_g)$, and as closed surfaces are classified by their Euler characteristic, we have the desired homeomorphicity. □

3.7 A discrete Poincaré-Hopf theorem

With the topology of S_σ and $\hat{\Sigma}_g$ established, we may now use some discrete geometry to show a discrete Poincaré-Hopf theorem for generic 1-chains τ. Note that we do not require τ to be harmonic in this case. Here, generic again refers to non-zero coefficients for each edge in Γ. For this, we utilize a discrete Gauss-Bonnet theorem.

3.7.1 Discrete Gauss-Bonnet

Let us briefly introduce discrete curvature and state the discrete Gauss-Bonnet theorem. We are considering discrete curvature for flat cone metrics on surfaces with boundary. For a cone point w in such a surface S, let $\theta(w)$, denote the angle sum at w. Then the discrete curvature at w is given by:

$$K_w := \begin{cases} 2\pi - \theta(w) & \text{if } w \notin \partial S, \\ \pi - \theta(w) & \text{if } w \in \partial S. \end{cases}$$

We may state the discrete Gauss-Bonnet theorem succinctly:

Theorem 3.7.1. For a flat cone metric on a surface with boundary S, we have the following formula holding:

$$\sum_{w \in W} K_w = 2\pi\chi(S)$$

The proof follows simply by a triangulation of the flat cone metric, decomposing it into Euclidean triangles.

3.7.2 Theorem and proof

Now we may go ahead and state and prove our discrete Poincaré-Hopf theorem:

Theorem 3.7.2. For a generic 1-chain τ on Σ_g with CW decomposition Γ, we have that:

$$\sum_{p \in P} Ind_\tau(p) = 2 - 2g$$

Proof. We consider a flat cone metric on a surface with boundary obtained by a partial closing of the boundary loops of $\hat{\Sigma}_g$. In this case, as we are dealing with a generic 1-chain τ, we assign a metric and squares s_i to $\hat{\Sigma}_g$ as in subsection 3.4.2, but we do it with respect to τ, as opposed to some harmonic 1-chain. For each given boundary loop, we still get a decomposition into 1-cells $l_1, l_2, \ldots, l_{2n}$ of alternating type, but the sum of the lengths of the even and odd 1-cells may not be equal.

For the partial closing, we take a 1-cell with smallest length $|l_{\min}|$, and we identify adjacent 1-cells along segments with length $\frac{|l_{\min}|}{3}$. More precisely, for each 1-cell l_i, we further decompose it into three 1-cells, labelling them in accordance with the cyclic order as t_{i_1}, t_{i_2}, and t_{i_3}. The first and third of these will have length $\frac{|l_{\min}|}{3}$, with the central 1-cell taking up the remainder of the length. Now, for each pair of adjacent 1-cells l_i and l_{i+1}, we identify t_{i_3} and $t_{(i+1)_1}$ in an isometric orientation-reversing manner. A boundary loop will remain, although it will be shortened. When the process is applied to each boundary loop, we get a surface with boundary, which we denote $\hat{\Sigma}_g^p$, along with a flat cone metric. It is clear that $\hat{\Sigma}_g^p$ is homotopic to $\hat{\Sigma}_g$.

For the resulting flat cone metric on $\hat{\Sigma}_g^p$, all the cone points are in the boundary, by construction. There is one for every pair l_i, l_{i+1} of partially identified edges, and its discrete curvature is $-\pi$, as it is the result of two squares being identified along part of

their respective sides. Thus, if we let P denote the set of vertices and faces in Γ, we have:

$$\begin{aligned} -\pi \sum_{p \in P} scg_\tau(p) &= 2\pi(2 - 2g - |V| - |F|) \\ \sum_{p \in P} 1 - \frac{scg_\tau(p)}{2} &= 2 - 2g \\ \sum_{p \in P} Ind_\tau(p) &= 2 - 2g \end{aligned}$$

□

If we return to considering harmonic 1-chains, recall that only boundary loops for vertices and faces of zero index have unique valid closings. In particular, if we are considering a surface of genus $g = 1$, then every boundary loop has a unique valid closing, and we get the corollary that our construction is unique in the $g = 1$ case.

Corollary 3.7.3. Given a topological torus T^2, a generic $[\sigma] \in H_1(T^2, \mathbb{R}) \setminus \{0\} = \mathbb{R}^2 \setminus \{0\}$, and a CW decomposition Γ with oriented edges, there exists a unique marked oriented square tiling of a flat cone metric d on T^2 that is associated with σ_h, the unique harmonic representative of $[\sigma]$ in the cellular homology.

3.8 A family of tilings

Earlier, we defined the discrete index of σ at a vertex or face p, and noted that there are multiple valid closings for boundary loops corresponding to vertices and faces of negative index. Here we make some conjectural remarks about this space of valid closings.

If the index is $-n$, then for a generic point in this space of valid closings, the image of the boundary loop will be a metric tree with all non-leaf vertices having degree four, and there will be n such vertices. At these non-leaf vertices, we may shift the partitioning of the segments at that vertex, giving us one dimension of freedom for each such vertex. We are currently working to obtain a precise description of this space of closings, so that we may prove the following conjecture:

Conjecture 3.8.1. For a boundary loop γ_p arising from a harmonic 1-chain σ, with $Ind_\sigma(p) = -n$, the space of valid closings forms a contractible n-dimensional CW complex.

Any associated tiling is obtained by making a choice of valid closing for each boundary loop, so the space of associated tilings is simply a product of the space of valid closings for each loop.

Conjecture 3.8.2. Given a closed, oriented surface of genus $g > 1$, a generic $[\sigma] \in H_1(\Sigma_g, \mathbb{R})\backslash\{0\}$, and a CW decomposition Γ with oriented edges, there exists a family of marked oriented square tilings of flat cone metrics d on Σ_g that is associated with σ_h, and this family forms a contractible $(2g-2)$-dimensional CW complex.

Chapter 4

Further Generalizations

In this chapter, we investigate three further generalizations, non-generic homology classes, tilings of surfaces with boundary, and rectangle tilings.

4.1 Non-generic $[\sigma]$

Recall that we referred to a $[\sigma] \in H_1(\Sigma_g, \mathbb{R})\backslash\{0\}$ as generic if its unique harmonic representative in the cellular homology with respect to Γ has non-zero coefficients for each edge. In this section, we investigate the case of non-generic $[\sigma]$, whose representatives have some zero coefficients. As noted in the introduction, we can still carry out our construction, but it may result in a tiling and flat cone metric on a surface of lower genus. Recall that V_0 and F_0 denote the vertices incident only to edges with zero coefficients and faces bounded only by edges with zero coefficients, respectively. A formula for this genus is given in terms of $|V_0|$, $|F_0|$, and the Euler characteristics of some graphs $\{H_j\}_{j=1}^{l}$ derived from the set of edges with zero coefficients. In this section, we prove Theorem 4.1.1:

Theorem 4.1.1. Given a closed, oriented surface Σ_g of genus $g \geq 1$, a non-generic $[\sigma] \in H_1(\Sigma_g, \mathbb{R})\backslash\{0\}$, and a CW decomposition Γ with oriented edges, there exists a marked oriented square tiling of a flat cone metric d on a surface S_σ of genus $g_0 \leq g$ that is associated with σ_h, the unique harmonic representative of $[\sigma]$. The genus g_0 is given by the formula:

$$g_0 = g + \frac{1}{2}\sum_{j=1}^{l}(\chi(H_j) - 1) + \frac{|V_0| + |F_0|}{2}$$

We begin with a description of the modified construction, and then introduce the $\{H_j\}_{j=1}^{l}$ and show that the formula holds. As in the previous chapter, all of our 1-chains in this section will be harmonic, so we denote them with σ, instead of σ_h, for greater simplicity.

4.1.1 Construction modifications

For the construction, we start again with Σ_g and a CW decomposition Γ, and use it to construct $\hat{\Sigma}_g$ by identification of discs. However, when we try to assign a metric to $\hat{\Sigma}_g$, we must be careful about the discs D_i that correspond to edges with zero coefficient, as we cannot assign a metric that will make the disc a point.

So, let E_0 denote the edges in Γ with zero coefficients, and we define another pinched surface $\hat{\Sigma}_g^o$, which is obtained from $\hat{\Sigma}_g$ by contracting (quotienting to a point, individually) all discs D_i for which $e_i \in E_0$. It is this contraction that can result in differing topology.

We then continue as before, assigning the metric d_σ by giving each D_i the geometry of a Euclidean square of side length $|c_i|$. This applies to edges in E_0 as well, whose corresponding discs are already points. In the same way as before, we also assign a marked oriented square of the same side length to each disc, with orientation specified by the direction of current flow along the edge. Note that for edges in E_0, the assigned square is a point with all marked points and sides coinciding, so discussion of orientation is irrelevant.

We again have the data of boundary loops, but note that if a vertex has all incident edges with zero coefficients, or a face has all boundary edges with zero coefficients, then its boundary loop will have contracted to a point in $\hat{\Sigma}_g^o$. Furthermore, vertices not in V_0 incident to an edge in E_0, or faces not in F_0 with a bordering edge in E_0, will have boundary loops with points that are marked squares of side length 0, corresponding to edges in E_0. As noted, for these marked squares of side length 0, their sides all coincide at the point square. Thus, the upshot is that this will not change the CW decomposition into an even number of 1-cells of alternating type.

By harmonicity, the boundary loops still have equal total lengths of 1-cells of opposite type, so we may apply valid closings to all those remaining to obtain a marked oriented square tiling of a closed surface, S_σ. As before, it is clear that we have a marked oriented square tiling, and for the structural correspondences, the images of the boundary loops under identification will be the horizontal and vertical segments. For vertices with all incident edges in E_0 and for faces with all boundary edges in E_0, their corresponding segments will be the points that their boundary loops have contracted to in the construction of $\hat{\Sigma}_g^o$.

4.1.2 Subgraph contraction and χ

Before we discuss the topology of the resulting S_σ from our construction, we present a simple lemma on the relationship between subgraph contraction and Euler characteristic for graphs. If we consider a finite graph G and a connected subgraph H, then the subgraph contraction is merely edge contraction performed on each edge of H. All of H is identified to a single vertex, and we call the resulting graph the quotient graph and denote it with G/H.

Lemma 4.1.2. For a finite graph G and a connected subgraph H, and the quotient graph G/H, we have the following relationship between their Euler characteristics:

$$\chi(G/H) = \chi(G) - \chi(H) + 1$$

Proof. Let V_G and E_G denote the number of vertices and edges of G. Similarly, let V_H and E_H, and $V_{G/H}$ and $E_{G/H}$ denote the number of vertices and edges of H and G/H, respectively. Then we see that $V_{G/H} = V_G - V_H + 1$ and $E_{G/H} = E_G - E_H$. Thus, $\chi(G/H) = (V_G - E_G) - (V_H - E_H) + 1 = \chi(G) - \chi(H) + 1$. □

More generally, we can consider the case of repeated contractions of multiple disjoint connected subgraphs $\{H_i\}_{i=1}^k$. Each component H_i is contracted to its own vertex, and we denote the result with $G/H_1/H_2/\ldots/H_k$.

Lemma 4.1.3. For a finite graph G and disjoint connected subgraphs $\{H_i\}_{i=1}^k$, and the quotient graph $G/H_1/H_2/\ldots/H_k$, we have the following relationship between their Euler characteristics:

$$\chi(G/H_1/H_2/\ldots/H_k) = \chi(G) - (\sum_{i=1}^{k} \chi(H_i)) + k$$

The proof is analogous to that of Lemma 4.1.2.

4.1.3 Topology of S_σ

We may now apply this lemma to the disc contractions performed on $\hat{\Sigma}_g$ to obtain $\hat{\Sigma}_g^o$. From this, we will be able to deduce the topology of S_σ, and prove the genus formula in Theorem 4.1.1. We begin by modeling the contractions as graph contractions, so that we may apply our lemma.

Consider a graph that is homotopic to $\hat{\Sigma}_g$, obtained by homotoping each disc D_i to an immersed cross subgraph. This graph has five vertices: one from the center of the disc and the four marked points on the boundary, and the edges are given by the line segments connecting the marked points to the center vertex. These cross subgraphs will usually be embedded, but in some instances some of the marked boundary points may be identified. We denote the union of the image of all these cross subgraphs with G_g.

Now, analogous to the disc contraction for edges in E_0, we may perform a contraction of the cross subgraphs for edges in E_0 to obtain a quotient graph that is homotopic to $\hat{\Sigma}_g^o$. If we consider the union of the cross subgraphs for edges in E_0, we may use $\{H_j\}_{j=1}^l$ to denote the connected components. Lemma 4.1.3 informs us that $\chi(\hat{\Sigma}_g^o) = \chi(\hat{\Sigma}_g) - (\sum_{j=1}^l \chi(H_j)) + l$.

To finish off the determination of the topology, we again use Lemma 3.6.1. Each valid closing that we perform is again homotopic to gluing in a disc by its boundary. However, note that the number of valid closings performed is no longer $|V|+|F|$, as certain boundary loops may have contracted to points, precisely those corresponding to vertices and faces

in V_0 and F_0.

Thus, we let $A = \hat{\Sigma}_g^o$ and let X be the space obtained after attaching discs to $\hat{\Sigma}_g^o$ (homotopic to S_σ), and we get a formula for the topology of S_σ in the non-generic case:

$$\begin{aligned}\chi(S_\sigma) &= \chi(\hat{\Sigma}_g) + \left(\sum_{j=1}^{l} 1 - \chi(H_j)\right) + (|V| - |V_0| + |F| - |F_0|) \\ &= \chi(\Sigma_g) + \left(\sum_{j=1}^{l} 1 - \chi(H_j)\right) - (|V_0| + |F_0|)\end{aligned}$$

A simple manipulation of the formula gives the formula for genus. Note also, that by the geometry of a marked square tiling, we know that it is impossible to obtain a genus 0 surface.

Proof that $g_0 \leq g$

As a final argument, we need to ensure that $g_0 \leq g$. This is equivalent to demonstrating that $\chi(S_\sigma) \geq \chi(\Sigma_g)$. Note first that if $V_0 = F_0 = \emptyset$, then it is clear. For any connected graph, the Euler characteristic is less than or equal to 1, so we get that $1 - \chi(H_j) \geq 0$ for all j.

When this is not the case, we must argue more carefully. Note that if we consider an element of V_0 or F_0, the cross subgraphs corresponding to the edges incident to a vertex, or bounding a face, belong to a particular connected subgraph H_j, as they all have zero coefficients. Let us further partition V_0 and F_0 into subsets $\{V_0^j\}_{j=1}^l$ and $\{F_0^j\}_{j=1}^l$, respectively, according to this membership. In particular, vertices in V_0^j are those whose incident edges have cross subgraphs that are in H_j. Faces in F_0^j are those whose bounding edges have cross subgraphs that are in H_j.

Then we may rewrite the Euler characteristic formula as follows:

$$\chi(S_\sigma) = \chi(\Sigma_g) + \left(\sum_{j=1}^{l} 1 - \chi(H_j) - |V_0^j| - |F_0^j|\right)$$

Thus, it will suffice to demonstrate for each j that the term $1 - \chi(H_j) - |V_0^j| - |F_0^j|$ is non-negative. This is equivalent to showing that $\text{rank}(H_1(H_j, \mathbb{R})) \geq |V_0^j| + |F_0^j|$.

Note first that each element of V_0 and F_0 has a boundary loop that is homotopic in $\hat{\Sigma}_g$ to a loop in one of the H_j. So, we just need to show that these loops are independent in $H_1(H_j, \mathbb{R})$ to show our desired inequality. For this, we consider an embedding of H_j in $\Sigma_{g,n}$ where $n = |V_0^j| + |F_0^j| + 1$. If the loops are independent in $H_1(\Sigma_{g,n}, \mathbb{R})$, then they will also be independent in $H_1(H_j, \mathbb{R})$.

The embedding of H_j will come from the embedding of G_g in Σ_g, with punctures added to create boundary components in accordance with V_0^j and F_0^j. In particular, for each vertex and face in these sets, add a boundary component, by excluding small open neighborhoods of the vertices and the centers of the faces. For the last boundary component, choose a face or vertex with a bounding or incident edge with non-zero coefficient. One must exist as $[\sigma] \neq 0$. Finally, we see that the boundary components corresponding to the vertices and faces in V_0^j and F_0^j are linearly independent from the following basic lemma from algebraic topology.

Lemma 4.1.4. If $b_1, \ldots, b_k$ are boundary components of a compact, orientable surface Y such that $\partial Y \neq \cup_{i=1}^k b_i$, then $[b_1], \ldots, [b_k]$ are linearly independent in $H_1(Y)$.

4.2 Surfaces with boundary

As noted in the introduction, we may also consider asking what happens when our 1-chain σ fails to be closed at a vertex, or co-closed at a face. In the interpretation of a 1-chain as current flow, this is analogous to introducing current sources and sinks at vertices or non-zero voltage sums around faces.

We may again carry out our construction and boundary components arise for each vertex or face at which the 1-chain fails to be harmonic. In this section, we first characterize what kinds of conditions on the vertices and faces are achievable by 1-chains, and refer to these conditions as *modified harmonic*. For such conditions, we may identify a unique 1-chain for each homological class, that we denote with σ_{mh}, though this identification is not canonical. Then we prove Theorem 4.2.1, as stated in the introduction:

Theorem 4.2.1. Given a closed, oriented surface Σ_g, a generic $[\sigma] \in H_1(\Sigma_g, \mathbb{R})\backslash\{0\}$, and a CW decomposition Γ with oriented edges, there exists a marked oriented square tiling of a flat cone metric d on $\Sigma_{g,n}$ that is associated with σ_{mh}, where n is the sum of the number of vertices and faces at which σ_{mh} fails to be harmonic.

4.2.1 Modified harmonicity

Recall the definitions and notation of Section 3.1. For a 1-chain σ, we have $\sigma = c_1 e_1 + \cdots + c_{|E|} e_{|E|}$ and $\phi_1(\sigma) = c_1 e_1^* + \cdots + c_{|E|} e_{|E|}^*$, where the e_i and e_i^* denote the edges and edge functionals of Γ. Also, we have $\partial\sigma = a_1 v_1 + \cdots + a_{|V|} v_{|V|}$ and $\delta\phi_1(\sigma) = d_1 f_1^* + \cdots + d_{|F|} f_{|F|}^*$, where v_j and f_k^* denote the vertices and face functionals of Γ.

These notations give us explicit linear maps $\partial : \mathbb{R}^{|E|} \to \mathbb{R}^{|V|}$ and $\delta : \mathbb{R}^{|E|} \to \mathbb{R}^{|F|}$ with the e_i, v_j, e_i^*, and f_k^* serving as bases for C_1^Γ, C_0^Γ, C_Γ^1, and C_Γ^2, respectively. We may direct sum these maps together to obtain one map $\partial \oplus \delta : \mathbb{R}^{|E|} \to \mathbb{R}^{|V|+|F|}$, and as Definition 3.1.1 states, a 1-chain is harmonic if it is in the kernel of $\partial \oplus \delta$.

We ask now for the image of $\partial \oplus \delta$, which will give us the space of *modified harmonic* conditions. This will tell us how we can ask σ to fail to be harmonic, at which vertices and faces, and by how much. Under the current interpretation for 1-chains, this is analogous to introducing source and sink vertices or faces in Γ.

Lemma 4.2.2.

$$\mathrm{im}(\partial \oplus \delta) = \{(a_1, \ldots, a_{|V|}, d_1, \ldots, d_{|F|}) \mid \textstyle\sum_{j=1}^{|V|} a_j = 0, \sum_{k=1}^{|F|} d_k = 0\}$$

Proof. Note that for a basis 1-chain e_i, we have that $\partial e_i = v_f - v_s$ where v_s and v_f denote the starting and ending vertices for e_i. The coefficients sum to 0, and so by linearity, we see that this will hold for any 1-chain. Note also that as the faces are oriented consistently, for any e_i, we have that $\delta\phi_1(e_i) = f_l - f_r$, where f_l and f_r denote the faces to the left and right of e_i. Thus, by linearity, the coeffients of $\delta\phi_1(\sigma)$ will sum to zero for any 1-cell σ. So, one inclusion is clear.

For the other inclusion, the homology and cohomology of Σ_g give us the result by

dimension considerations. As $H_0^\Gamma(\Sigma_g, \mathbb{R}) = \mathbb{R}$, $\mathrm{im}(\partial)$ is precisely the space of 0-chains with coefficients that sum to zero. Similarly, as $H^2_\Gamma(\Sigma_g, \mathbb{R}) = \mathbb{R}$, $\mathrm{im}(\delta)$ is precisely the space of 2-cochains with coefficients that sum to zero. □

Recall that the kernel of $\partial \oplus \delta$ denotes the space of harmonic 1-chains, and is of dimension $2g$. Thus, this tells us that for a modified harmonic condition, there will be a $2g$-dimensional space of 1-chains that satisfy them. There is no canonical choice of identification between a homology class and a solution, but we may choose one by projecting orthogonally to the kernel (with respect to the metric given by taking the e_i as an orthonormal basis). As stated earlier, we will denote this 1-chain with σ_{mh}.

Lastly, we note that we again restrict to generic modified harmonic 1-chains with all coefficients being non-zero. Consideration of non-generic modified harmonic 1-chains leads to predictably more complicated results, and we leave those aside in this thesis.

4.2.2 Associated square tilings of surfaces with boundary

Before we can proceed, we must define a marked oriented square tiling on a surface with boundary, and what it means for it to be associated with a modified harmonic 1-chain σ_{mh}.

Definition 4.2.3. A *marked oriented square tiling* of a flat cone metric d on a compact, oriented, connected surface $\Sigma_{g,n}$ is a covering by marked squares $s_1, s_2, \ldots, s_m$, with disjoint interior so that:

$$\left(\bigcup_{i=1}^{m} s_i^t\right) \setminus \partial\Sigma_{g,n} = \left(\bigcup_{i=1}^{m} s_i^b\right) \setminus \partial\Sigma_{g,n}$$
$$\left(\bigcup_{i=1}^{m} s_i^l\right) \setminus \partial\Sigma_{g,n} = \left(\bigcup_{i=1}^{m} s_i^r\right) \setminus \partial\Sigma_{g,n}$$

Additionally, we require that each boundary component be a subset of one of the four set unions above.

The last condition ensures that boundaries are only of one "type", and consist of only sides of one type, though again this is not strictly true, so we have stated it as given. Note

also that with this definition, it is clear that any cone points on the boundary will have cone angles in $\pi + 2\pi\mathbb{N}$.

Now for the definition of such a tiling being associated with a modified harmonic 1-chain. We adopt similar notation as that in subsection 3.2.2. Furthermore, to shorten the statement, particularly in conditions 2 and 3, we assume that the edges are oriented such that all coefficients are non-negative. We may do this, as these assignments are arbitrary, and are simply made for the purpose of explicit ∂ maps.

Definition 4.2.4. A marked oriented square tiling of a flat cone metric d on a surface $\Sigma_{g,n}$ will be *associated* to σ_{mh} if two sets of conditions are met. First, the following correspondences must hold:

1. Each edge e_i corresponds to a marked square s_i with side length $|c_i|$.
2. Each vertex v corresponds to a horizontal segment h_v with length $\max\left(\sum_{e\in\mathcal{I}(v)} c_i, \sum_{e\in\mathcal{O}(v)} c_i\right)$.
3. Each face f, with boundary loop denoted ∂f, corresponds to a vertical segment u_f with length $\max\left(\sum_{e\in\mathcal{F}(\partial f)} c_i, \sum_{e\in\mathcal{B}(\partial f)} c_i\right)$.

Secondly, the tiling must reflect the topology of Γ and σ_{mh}.

4. If an edge e_i carries current flowing out of (into) vertex v, then the bottom (top) side of s_i is contained in h_v.
5. If an edge e_i is carrying current clockwise (counterclockwise) about face f, then the right (left) side of s_i is contained in u_f.

The changes to conditions 2 and 3 account for the existence of boundary components that may be part of these horizontal and vertical segments. In particular, we will seee that if σ_{mh} fails to be closed or co-closed at a vertex or face, respectively, then the length of the corresponding boundary component in the resulting flat metric will be equal to the magnitude of this failure. If it is a vertex, the boundary component will be part of a horizontal segment, and if it is a face, it will be part of a vertical segment.

4.2.3 Boundary loop closings

We now may proceed with the proof of Theorem 4.2.1 by construction. We again construct $\hat{\Sigma}_g$ in the same fashion, and assignment of $d_{\sigma_{mh}}$ can be done analogously, with boundary loops arising for each vertex and face. We again decompose them into an even number of 1-cells that consist of sides of one type, which alternates as you traverse the loop. We again use l_i denote these 1-cells and $|l_i|$ to denote their lengths.

Note now that with the modified harmonic condition, we no longer have that total lengths of the 1-cells grouped by type are equal. In particular, if our modified harmonic condition at vertex v_j requires that the coefficient for $\partial\sigma_{mh} = a_j$, then we will have that $|l_1| - |l_2| + |l_3| - \cdots - |l_{2n}| = a_j$, assuming we started labelling with a 1-cell consisting of tops of squares. An analogous statement holds for faces.

In order to close these boundary loops, we must make slight modifications to the definitions in subsection 3.5.2. Again, we let p denote either a vertex or a face, and we use a_p to denote the desired coefficient for that vertex or face functional in the modified harmonic condition.

Definition 4.2.5. An *open loop closing* of a boundary loop γ_p will be a further decomposition of the $\{l_i\}_{i=1}^{2n}$ into 1-cells $\{t_j\}_{j=1}^{2m+1}$, the last of which is of length $|a_p|$, and a pairing of the first $2m$ 1-cells of opposite type, designating an orientation-reversing isometric identification of those paired segments.

We again would like to avoid the introduction of additional genus with a closing. As before, let us embed γ_p in $\mathbb{R}^2$ as the boundary of a disc centered at the origin, and remove the interior of said disc, and consider the resulting topology when the identifications are made.

Definition 4.2.6. A *valid open closing* of a boundary loop γ_p will be an open loop closing which results in a space with the topology of $\mathbb{R}^2 \setminus \mathbb{D}$, when γ_p is embedded as suggested above.

Again, we have two equivalent conditions. The first is that the image of the identified

1-cells (so all but the last one) will be a metric tree under the quotient map of the identification. A boundary loop of length $|a_p|$ will remain corresponding to this last unidentified 1-cell. The second is the same as before: if two pairs of points (x_1, x_2) and (y_1, y_2) on γ_p are identified, then the lines between them must not cross when considered in the embedding into the plane.

We may prove existence of valid open closings in a manner analogous to the procedure in the proof of Lemma 3.5.4.

Lemma 4.2.7. For any boundary loop γ_p arising from a modified harmonic 1-chain σ_{mh}, there exists a valid open closing.

The proof is omitted, due to this similarity. We apply these valid open closings to each boundary loop to obtain a marked oriented square tiling of a surface $S_{\sigma_{mh}}$. To determine the topology, we again use Lemma 3.6.1.

Lemma 4.2.8. $S_{\sigma_{mh}}$ is homeomorphic to $\Sigma_{g,n}$, where n is the number of vertices and faces where the modified harmonic condition asks that being closed or co-closed fails.

Proof. Let V_m and F_m denote the vertices and faces, respectively, where the modified harmonic condition differs from the typical harmonic condition. Then, as before, for each vertex or face where σ_{mh} is still harmonic, a valid closing is homotopic to gluing in a disc. At vertices and faces in V_m and F_m, valid open closings leave boundary components, and no change is made, up to homotopy. As such, we apply Lemma 3.6.1 with X being the space with disc attachments (homotopic to $S_{\sigma_{mh}}$), and $A = \hat{\Sigma}_g$ and find that $\chi(S_{\sigma_{mh}}) = -|E| + (|V| - |V_m|) + (|F| - |F_m|) = \chi(\Sigma_g) - (|V_m| + |F_m|)$. □

As a final note, we mention that the classical result may be obtained as a special case, if we consider the embedded planar electrical network as a CW decomposition of $\Sigma_0 = \mathbb{S}^2$ (the compactification of the plane). We consider the modified harmonic condition where co-closure fails at the faces with b as a bounding edge, and the result of our construction is an associated square tiling and flat cone metric on a cylinder $\Sigma_{0,2}$. This tiling is the

same as the tiling from the classical result if we remove the square corresponding to the battery edge.

4.3 Rectangle tilings

In this short section, we briefly describe the necessary modifications to achieve rectangle tilings. In general, this entails adding the data of a non-unit resistance on each edge, which gives the aspect ratio of the corresponding rectangle.

4.3.1 The classical case

In the classical case, we may define a *general planar electrical network*, which includes the additional data of a resistance function on each non-battery edge.

Definition 4.3.1. A *general planar electrical network* is a quadruple (G, b, Y, r) consisting of a planar, connected, directed graph G, a non-loop edge $b \in G$ to designate the battery edge, a number $Y \in \mathbb{R}$ to denote the voltage to be applied over b, and a function $r : E \backslash \{b\} \to \mathbb{R}^+$ describing the resistance of each non-battery edge.

With the addition of this data, we must briefly generalize Kirchhoff's laws.

Kirchhoff's laws

To state them more generally, we define an additional function on the edges $d : E \to \mathbb{R}$, which describes the voltage drop over each edge. With voltage Y being applied over the battery edge b, we have that $d(b) = Y$.

With this new function, Ohm' s law becomes simpler to state: for all non-battery edges $e \in E \setminus \{b\}$, we have $d(e) = c(e)r(e)$. The current law remains unchanged. The voltage loop law is stated with the voltage drop function replacing the current function, as they are no longer equal due to non-unit resistances:

$$\sum_{e \in \mathcal{F}(\gamma)} d(e) = \sum_{e \in \mathcal{R}(\gamma)} d(e)$$

With Ohm's law, it is clear that the voltage loop law may be described in terms of the current and resistance functions, so we may speak simply of searching for an appropriate current function c as the solution to Kirchhoff's laws. The proof of existence and uniqueness of this function remains the same.

Associated rectangle tilings

There is an obvious modification of the definition for a square tiling of a rectangle into a rectangle tiling of a rectangle.

Definition 4.3.2. A *rectangle tiling of a rectangle* is a covering by rectangles with disjoint interiors, of a Euclidean rectangle with designated top, bottom, left, and right sides.

Let us also make the proper modifications to Definition 2.4.1 to obtain the definition for a rectangle tiling to be *associated* with a general planar electrical network.

Definition 4.3.3. We say that a rectangle tiling is *associated* to a circuit solution c of a general planar electrical network if two sets of conditions are met. First, the following correspondences must hold:

1. Each resistor edge e corresponds to a rectangle q_e with width $|c(e)|$ and height $|d(e)| = r(e)|c(e)|$.

2. Each vertex v corresponds to a horizontal segment h_v with length $\sum_{e\in\mathcal{I}(v)} c(e) = \sum_{e\in\mathcal{O}(v)} c(e)$, the total current through v.

3. Each face f whose boundary consists of resistor edges (forming a simple loop denoted ∂f), corresponds to a vertical segment u_f with length $\sum_{e\in\mathcal{F}(\partial f)} r(e)c(e) = \sum_{e\in\mathcal{R}(\partial f)} r(e)c(e)$.

Secondly, the tiling must reflect the topology of Γ and the circuit solution. In the following conditions, note that the sign of $c(e)$ in conjunction with the direction on e will determine the direction of current flow.

4. If an edge e carries current flowing out of (into) vertex v, then the bottom (top) side of q_e is contained in h_v.

5. If an edge e is carrying current clockwise (counterclockwise) about face f, then the right (left) side of q_e is contained in u_f.

Then we get the following result:

Theorem 4.3.4. Given a general planar electrical network (G, b, Y, r) with a unique circuit solution $c : E \setminus \{b\} \to \mathbb{R}$, and a fixed embedding of G in the plane, there is a unique associated rectangle tiling of a rectangle of height Y and width I, the total current through the network.

The proof follows with almost no modification, and this result is mentioned in [BSST].

4.3.2 The general case

As before, we begin with a closed, oriented, connected surface of genus $g \geq 1$ with a CW decomposition Γ. In addition, we now have a function $r : E \to \mathbb{R}^+$ assigning a resistance to each edge. Given a non-zero homological class $[\sigma] \in H_1(\Sigma_g, \mathbb{R})\backslash\{0\}$, we will again have a unique harmonic representative $\sigma_h \in C_1^\Gamma(\Sigma_g, \mathbb{R})$ in the cellular homology with respect to Γ.

Harmonicity

As Kirchoff's laws required modification and generalization, we must also generalize the definition of harmonic, with the additional resistance data. As before, recall the typical setup for cellular homology and cohomology and the ∂ and δ operators.

$$\begin{array}{ccccc} C_0^\Gamma & \xleftarrow{\partial} & C_1^\Gamma & \xleftarrow{\partial} & C_2^\Gamma \\ & & \downarrow{\scriptstyle \phi_1} & & \\ C_\Gamma^0 & \xrightarrow{\delta} & C_\Gamma^1 & \xrightarrow{\delta} & C_\Gamma^2 \end{array}$$

Previously, we defined ϕ_1 to take e_i to e_i^*. The data of the resistance function will change this definition. In particular, we define $\phi_1(e_i) := r_i e_i^*$ (where r_i is shorthand for

$r(e_i)$) and extend to all 1-chains by linearity. With this change to ϕ_1, there is no need to change the statement of the definition of harmonicity, though the condition is clearly more general.

Definition 4.3.5. A 1-chain $\sigma \in C_1^\Gamma$ is *harmonic* if $\partial\sigma = 0$ and $\delta\phi_1(\sigma) = 0$. In other words, if σ is both closed and co-closed.

As before, a harmonic 1-chain σ may be thought of as a local solution to Kirchhoff's laws generalized to accomodate non-unit resistances. For this, we still consider the coefficients c_i as describing the current through each edge. With this, it is clear that $\partial\sigma = 0$ still corresponds to the current law holding at each vertex, in the same way as it did before.

For the condition $\delta\phi_1(\sigma) = 0$, we will see that our redefinition of ϕ_1, leads to this being analogous to Ohm's law and the voltage loop law holding around each face. Again, let $\delta\phi_1(\sigma) = d_1 f_1^* + \cdots + d_{|F|} f_{|F|}^*$, where the f_k^* denote the face functionals in C_Γ^2. Then, we may express the coefficient d_k as the total voltage drop around f.

$$d_k = \left(\sum_{e_i \in \mathcal{F}(\gamma)} c_i r_i \right) - \left(\sum_{e_i \in \mathcal{B}(\gamma)} c_i r_i \right)$$

Within this expression, we see that we are summing the local voltage drops as our terms are the products of the currents and resistances. This is the manifestation of Ohm's law.

For the proof of a unique harmonic representative, we have the exact same proof, except that we take the $r_i e_i$ as a basis. The proof follows verbatim, otherwise.

Lemma 4.3.6. For a homological class $[\sigma] \in H_1^\Gamma(\Sigma_g)$, there is a unique harmonic representative σ_h.

For this section, we only discuss generic σ with non-zero coefficients. The non-generic results are easily modified, so we leave those results unstated.

Associated rectangle tilings

Let us generalize the appropriate tiling-related definitions. The tilings that are produced consists of *marked rectangles* which are Euclidean rectangles with designated top, bottom, left, and right sides. Analogous to previous notation, we denote these sides of a rectangle q_i in a tiling with q_i^t, q_i^b, q_i^l, and q_i^r, respectively. A marked rectangle in a surface with a flat cone metric is defined to be the image of a continuous map on a marked rectangle which is an isometric embedding on the interior.

Definition 4.3.7. A *marked oriented rectangle tiling* of a flat cone metric d on a closed, oriented surface Σ_g is a covering by marked rectangles $q_1, q_2, \ldots, q_m$, with disjoint interior so that:

$$\bigcup_{i=1}^{m} q_i^t = \bigcup_{i=1}^{m} q_i^b \quad \& \quad \bigcup_{i=1}^{m} q_i^l = \bigcup_{i=1}^{m} q_i^r$$

The definition for an associated rectangle tiling is modified just as it is in the classical case. We include the definition for completeness.

Definition 4.3.8. A marked oriented rectangle tiling of a flat cone metric d on a surface S_g will be *associated* to σ_h if two sets of conditions are met. First, the following correspondences must hold:

1. Each edge e_i corresponds to a marked rectangle q_i with height $r_i|c_i|$ and width $|c_i|$.
2. Each vertex v corresponds to a horizontal segment h_v with length $\sum_{e\in\mathcal{I}(v)} c_i = \sum_{e\in\mathcal{O}(v)} c_i$, the total current through v.
3. Each face f, with boundary loop denoted ∂f, corresponds to a vertical segment u_f with length $\sum_{e\in\mathcal{F}(\partial f)} c_i r_i = \sum_{e\in\mathcal{B}(\partial f)} c_i r_i$.

Secondly, the tiling must reflect the topology of Γ and σ_h. In the following conditions, recall that the sign of c_i in conjunction with the direction on e_i will determine the direction of current flow.

4. If an edge e_i carries current flowing out of (into) vertex v, then the bottom (top) side of q_i is contained in h_v.

5. If an edge e_i is carrying current clockwise (counterclockwise) about face f, then the right (left) side of q_i is contained in u_f.

The result

We may now state our result for rectangle tilings:

Theorem 4.3.9. Given a closed, oriented surface Σ_g of genus $g \geq 1$, a generic $[\sigma] \in H_1(\Sigma_g, \mathbb{R})\backslash\{0\}$, a CW decomposition Γ with oriented edges, and a function $r : E \to \mathbb{R}^+$, there exists a marked oriented rectangle tiling of a flat cone metric d on Σ_g that is associated with σ_h.

The proof is analogous to the previous one, so we omit discussion.

Finally, as we've hinted at a few times, we may combine any subset of the three generalizations just discussed to obtain more complicated statements, but we have decided to avoid such an exercise, for the sake of the reader.

References

[BSST] Brooks, R. L.; Smith, C. A. B.; Stone, A. H.; Tutte, W. T. The dissection of rectangles into squares. Duke Math. J. 7, (1940). 312-340.

[CL] Chien, E.; Luo, F. Rectangular tilings of surfaces, in preparation.

[CLS] Chien, E.; Luo, F.; Savas, M. Ptolemy's and Casey's theorems in Minkowski and de Sitter geometries, in preparation.

[Cal] Calegari, D. (2013). Kenyon's squarespirals. Geometry and the imagination [web log]. Retrieved Sep. 2014, from http://lamington.wordpress.com/2013/01/13/kenyons-squarespirals/

[CFP] Cannon, J. W.; Floyd, W.J.; Parry, W.R. Squaring rectangles: the finite Riemann mapping theorem. Contemporary Mathematics. 169, (1994), 133-212.

[CS] Chelkak, Dmitry; Smirnov, Stanislav Discrete complex analysis on isoradial graphs. Adv. Math. 228 (2011), no. 3, 1590-1630

[De] Dehn, Max. Über Zerlegung von Rechtecken in Rechtecke. (German) Math. Ann. 57 (1903), no. 3, 314-332.

[DU] Gu, Xianfeng (David); Luo, Feng; Sun, Jian; Wu, Tianqi, A discrete uniformization theorem for polyhedral surfaces, arXiv:1309.4175 [math.GT].

[H1] Hersonsky, S. Boundary Value Problems on Planar Graphs and Flat Surfaces with Integer Cone singularities I; The Dirichlet problem, J. Reine Angew. Math. 670, (2012), 65-92.

[H2] Hersonsky, S. Boundary Value Problems on Planar Graphs and Flat Surfaces with Integer Cone singularities II; Dirichlet-Neumann problem, Differential Geometry and its Applications. 29, (2011), 329-347.

[H3] Hersonsky, S. Combinatorial Harmonic Maps and Convergence to Conformal Maps, I: A Harmonic Conjugate, Commentarii Mathematici Helvetici.

[H4] Hersonsky, S. Combinatorial Harmonic Maps and Convergence to Conformal Maps, II: Convergence and Moduli, in preparation.

[K] Kenyon, R. Tiling with squares and square-tileable surfaces, preprint.

[Ma] Masur, Howard. Ergodic theory of translation surfaces. Handbook of dynamical systems. Vol. 1B, 527-547, Elsevier B. V., Amsterdam, 2006.

[MT] Masur, Howard; Tabachnikov, Serge Rational billiards and flat structures. Handbook of dynamical systems, Vol. 1A, 1015-1089, North-Holland, Amsterdam, 2002.

[M1] Mercat, Christian. Discrete Riemann surfaces and the Ising model. Comm. Math. Phys. 218 (2001), no. 1, 177-216.

[M2] Mercat, Christian. Discrete Riemann surfaces. Handbook of Teichmller theory. Vol. I, 541-575, IRMA Lect. Math. Theor. Phys., 11, Eur. Math. Soc., Zrich, 2007.

[P] Poincaré, Henri. The Value of Science. Dover, New York, 1958.

[S] Schramm, Oded. Square tilings with prescribed combinatorics. Israel J. Math. 84 (1993), no. 1-2, 97-118.

[CP] Stephenson, Kenneth. Introduction to circle packing. The theory of discrete analytic functions. Cambridge University Press, Cambridge, 2005.

[Z] Zorich, Anton. Flat surfaces. Frontiers in number theory, physics, and geometry. I, 437-583, Springer, Berlin, 2006.